ABSTRACT

Mohamed, Tarek Said. ***Fabrication and Analysis of Three-Dimensionally Reinforced Cellular Matrix Composites Foamed by Chemical Blowing Agent*** (Under the direction of Dr. Yiping Qiu).

The objective of this research was to investigate the process of three-dimensional textile reinforced cellular matrix composites (3DCMC) and propose it to the industry.

The scope of this research involved shortening the production cycle of 3DCMC foamed by a physical blowing agent, investigating the potential of using a chemical blowing agent to foam the structure instead of a physical blowing agent, and finally test the mechanical properties of the structures made by the optimum condition.

Using the high pressure foaming apparatus, experiments were conducted by manipulating production parameters, to investigate the possibility of shortening production time. The production time was successfully reduced from twenty hours to six hours. At this point, two problems remained unsolved, the high cost of the equipment and the danger associated with using the equipment. This led to the search for applying a chemical blowing agent to fabricate 3DCMC. A comprehensive review of the literature was done to study the idea behind foaming by chemical blowing agents. Several experiments were conducted by using Thermal Gravitational Analysis (TGA) to study the decomposition behavior of chosen blowing agents. Sodium bicarbonate was chosen as a blowing agent.

Composite samples were fabricated using six different concentrations of sodium bicarbonate.

An optimum concentration of 5% was chosen to be applied on composite samples and the mechanical properties of those composite samples were tested and compared to 3DRMC. A four point bending test, tensile test, and drop weight impact test were conducted on each sample to evaluate the performance of the fabricated composites. The flexural strength of both 3DCMC and 3DRMC was almost the same, while the tangent modulus of 3DCMC was higher than 3DRMC. There was no significant difference in tensile strength between 3DCMC and 3DRMC. 3DCMC had higher impact energy absorption than 3DRMC at the low impact velocity of 3 m/s, which makes 3DCMC attractive to applications that requires high impact resistance and low density.

Fabrication and Analysis of Three-Dimensionally Reinforced Cellular Matrix Composites Foamed by Chemical Blowing Agent

by

Tarek Said Mohamed

A Thesis Presented to the Faculty of the Graduate School

of North Carolina State University

in Partial Fulfillment of the Requirements for the Degree of

Master of Science

Textile Engineering

Raleigh

2002

APPROVED BY

_____	_____
Dr. Jon Rust	Dr. Traci May-Plumlee

_____

Dr. Yiping Qiu

Chair of Advisory Committee

TO MY FAMILY

BIOGRAPHY

Tarek Mohamed was born in Alexandria, Egypt, in July 1977. He received his high school diploma in the summer of 1995. In the fall of 1995, he began his undergraduate education, at the Arab Academy for Science and Technology, in Alexandria. He joined the department of Construction and Building Engineering. In the fall of 1997, he decided to transfer to Auburn University, to pursue his B.S Degree in Textile Engineering.

In March 2000, he earned his B.S Degree in Textile Engineering from Auburn University. Due to his great interest in research and in the composite field, he decided to join the graduate school upon receiving his B.S Degree. In the fall of 2000, he joined the College of Textiles at North Carolina State University, to work towards his M.S degree in Textile Engineering with an emphasis in composites.

During his graduate studies in the College of Textiles, he has been working on improving the production of 3DCMC. Tarek was able to develop a new procedure, which successfully fabricated 3DCMC with lower cost and high speed production.

ACKNOWLEDGEMENT

In the journey toward the completion of this thesis, the author has been greatly thankful to seven respectful individuals, who always encouraged him in academic endeavors: his mother, his father, his uncle, his fiancé, his brother and sisters.

Dr. Yiping Qiu, Chair of advisory committee, Dr. Jon Rust and Dr. Traci May-Plumlee, members of his advisory committee deserve special recognition for their guidance and patience throughout the research. The author is thankful to Dr. Qiu for providing him the opportunity to work on the fascinating project of 3DCMC.

The author would like to thank 3TEX, Inc of Cary, NC for providing a grant to assist in carrying on this project, and for providing the necessary samples for the experiment.

Appreciation is extended to the following professors at North Carolina State University: Dr. Mohammed Zikry, Department of Mechanical and Aerospace Engineering, for assistance with the impact tests, Dr. Fuh-Gwo Yuan, of the Mars Mission Research Center for permitting access to MMRC lab.

The author would also like to explore his sincere thanks to Mr. Chuyang Zhang, Ph.D. student at College of Textiles, for the tensile test samples, and Mr. Jared Baucom, Ph.D. student at Department of Mechanical and Aerospace Engineering, for impact test samples, Mr. Pankaj Agrawal for assistance with using strain gages, and Mr. Stanon Batchelor for assistance using the pressure vessel.

The author is also thankful to Dr. Zaisheng Cai, a post doctorate from China and his group mates, Ms. Anshu Dixit, Mr. Nagendra Anantharamaiah, Mr. Chaithanya Renduchintale, Ms. Chris Jenson, Mr. Brice Langston for their helpful suggestions on the presentation.

TABLE OF CONTENTS

LIST OF TABLES

LIST OF FIGURES

1. INTRODUCTION

Composite materials have unique properties, which are superior than those of conventional materials such as metals and ceramics. Those unique properties are attained by the combination of two or more materials with different properties.

Modern composites can be classified by matrix material (polymer matrix, metal matrix, and ceramic matrix), by processing or by function. Composite materials have a combined set of superior properties, which make them more attractive than other materials.

Textile reinforced composites have been widely used. Textile composites are formed by impregnating the resin matrix with textile preform, in the form of fibers, yarns or fabrics. Applications for fibrous reinforced composites have been increasing dramatically the past decade, due to their high strength and modulus. Two-dimensional (2D) composites have poor properties in the thickness direction. Three-dimensional (3D) woven composites demonstrate better structural integrity, as their delamination is not possible.

Reducing the density of 3D composites makes them more desirable and broadens their applications. Several studies were performed to reduce the density of 3D composites without having a negative effect on their mechanical properties. The last stage of this study was reached by Xu, et al [1]. They successfully foamed the epoxy matrix by nitrogen gas as a physical blowing agent. The resin pockets were replaced by microcells, and resulted in 28-37% reduction in density. However the process remains very expensive and slow, limiting opportunities for its use in industry.

1.1 Justification

The innovation of 3DCMC succeeded in reducing the density of composites . Therefore, lightweight and high strength composites were fabricated. On the other hand, there are many disadvantages associated with this technology. The production time is too long (20 hours process) and the process is dangerous and expensive. Therefore, the industry would not adopt the process with all these disadvantages. This project aims to modify and optimize the process and reduce or eliminate the disadvantages.

1.2 Objectives

The goal of this project was to investigate the 3DCMC process. This study aimed to shorten the production time by the determination of the optimum process using the physical blowing agent and by using an appropriate chemical blowing agent. The goals of this project were also extended to reducing the cost of the process and eliminating the danger associated with the process.

1.3 Approach

The plan taken to achieve the ideal final results can be divided into two parts. The first part was to investigate the effect of reducing the saturation time by manipulating the parameters involved in the process, then to calculate density and fiber volume fraction of composites fabricated under each condition tested. The second part was to investigate the potential for using a chemical blowing agent instead of a physical blowing agent. Different concentrations of the chemical blowing agent will be applied in order to control the density, then fiber volume fraction was calculated for composites fabricated under each condition.

The best condition was selected, and a thorough comparison was done between the selected production parameters and the control (3DRMC). The comparison included density, fiber volume fraction, and the mechanical performance of each of the following: flexural strength, tangent modulus, tensile strength, tensile modulus, and impact resistance.

2. REVIEW OF LITERATURE

2.1 Composite Structures

A composite material is composed of two or components with different properties. The woven preform composite materials have significant variation in properties when measured in different directions. Composite materials may be classified according to matrices, fibers and mechanical properties.

Fiber reinforced composite materials enjoy several advantages which include their high strength to weight ratio, high stiffness to weight ratio, high fatigue resistance, absence of catastrophic failure and low thermal expansion in fiber oriented directions [27]. The major component of fiber reinforced composites are fibers, which share the major portion of the load. The matrix material protects the surface of the fibers and transfers stress between them. Coupling agents and coatings prevent reaction between fibers and matrix. Finally fillers and other additives reduce the cost and increase stiffness [27].

2.1.1 Reinforcing Fibers Used in Composites

The most frequently used fibers in composites are carbon, glass, aramid, and Spectra ®. Carbon fibers encompass a wide spectrum of advantages including their high strength and modulus, resistance to corrosion, high heat resistance, high strength at elevated temperatures and low density. However, carbon fibers are brittle and expensive [27]. Glass is denser than carbon and has a lower modulus. The strength and modulus of these fibers are determined by their atomic structure. Glass is divided into three types: E glass, C glass, and S glass. E glass has lower cost, and good strength and stiffness. Glass fibers are isotropic (i.e. the axial and

transverse young's moduli are the same). The strength is strongly dependent on processing conditions. The diameter of E glass is between 8 and 15 μm [27].

Aramid fibers consist of polyamide with benzene rings between amide groups. Aramid fibers are highly anisotropic with high strength and modulus, low density and high temperature resistance but poor transverse properties [27]. Spectra ® fibers have a linear molecular structure and high crystallinity. Spectra ® fibers has a low glass transition temperature and low melting temperature. There are several advantages for Spectra® fibers, which include their high strength and modulus, low density and excellent resistance to chemicals. However, several features such as poor adhesion to the matrix and high creep due to the low intermolecular forces, prevent them from being used in many applications.

2.1.2 Matrices Used in Composites

Matrices are categorized into three categories: polymeric, ceramic and metallic. Polymeric matrices are classified into two classes: thermoplastic and thermosetting. Thermoplastic resins do not cross-link. They have high failure strain, high impact resistance, unlimited storage life, short fabrication time, and low creep resistance [27].

Properties of thermosetting resins depend on their molecular structure and crosslinking density. Thermosetting resins have less creep and stress relaxation, good resistance to heat and chemicals, and good wet out between fibers and matrix. However, thermosets require a long time to cure and have low impact resistance [27]. This class of matrices includes epoxies, unsaturated polyesters and vinyl esters.

Epoxy resin is classified into two classes, prepolymers (reactive epoxy group) and cured resin (no epoxy group) [27]. During curing, epoxy reacts with the curing agent, known as hardener, and as curing is carried out, the molecular weight of the polymer increases as well as the glass transition temperature.

There are several stages that are reached during the curing of thermosetting resins. Figure 2.1 shows the schematic time-temperature-transformation diagram of epoxy resin [17]. The stages include phase separation, gelation, vitrification, full cure, and devitrification [17]. The phase separation stage is when precipitation of rubber occurs. Gelation corresponds to the incipient formation of an infinite molecular network, which gives rise to long range elastic behavior in the macroscopic fluid. After this stage, the material consists of sol (soluble fraction) and gel (insoluble fraction). After the gel point is reached, the viscosity of the resin starts to increase. Therefore, the gel increases and the sol decreases. Vitrification occurs when the glass transition temperature rises to the isothermal temperature of the cure [17].

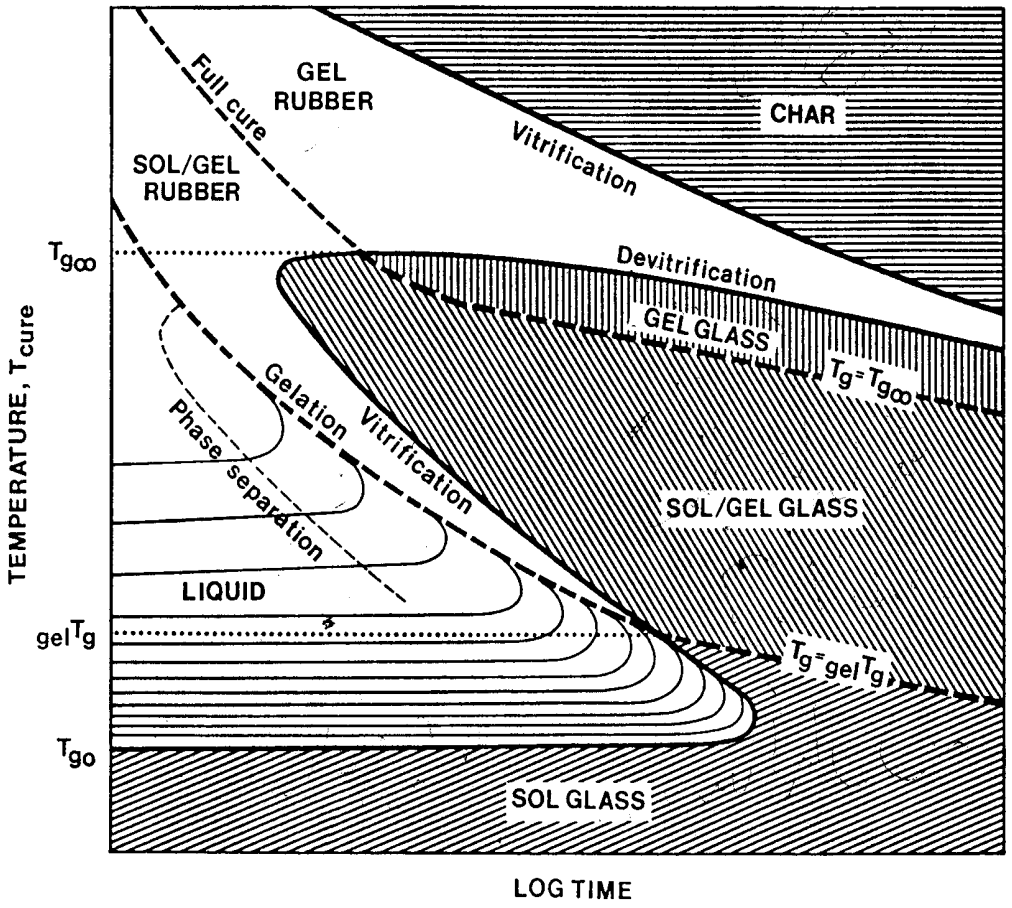

Figure 2.1 Time-Temperature-Transformation Diagram of Epoxy Resin [17]

2.1.3 Fabric Geometry Used in Composite Preforms

Several fabric structures may be used to fabricate textile composites, for example, unidirectional, two-dimensional (which may be woven or nonwoven), and three-dimensional (orthogonal, multidirectional, knitted and braided). Two-dimensional woven fabric offers high fiber volume fraction, and high strength and modulus in both directions. However, 2D fabric preforms may not be capable of producing complex shapes. Nonwoven preforms have the highest productivity rate. They also have the same low strength and modulus in all directions, and low fiber volume fraction [27].

2.1.4 Properties of 3D Composites

A study was conducted [15] to compare the mechanical performance of 3D woven carbon-carbon composites with advanced carbon-carbon laminated composites. It was found that, in the thickness direction, 3D woven composites had three times the shear strength of advanced carbon-carbon laminated composites, twice the tensile strength, and 65% higher flexural strength.

A comparison of 3D woven carbon-epoxy composites with aluminum, was studied [13, 15]. Tensile strength and modulus of elasticity were compared for both materials. 3D woven composites held higher values. This study concluded that 3D composites could be used in aircraft and space applications.

Gu [16] found that 2.8% is an optimum percentage for fiber volume fraction in the z-direction. He concluded that increased z yarn size has negative effect on tensile strength.

2.2 The Foaming Process

2.2.1 Steps Involved in the Foaming Process

Foaming may be summarized in a few steps. The first step is the generation of a great number of microcells. The second step is the growth of the generated microcells, as gas released through the polymer. The generated microcells grow until the viscosity of the resin increases to an extent that the cells can no longer grow. At this point, microcells are stabilized. For thermosets, increasing the viscosity is achieved through an irreversible crosslinking reaction, while for thermoplastic resins increasing the viscosity is achieved by cooling [22, 34, 36].

2.2.2 Foaming Products

Foaming of plastics is relatively easy, and makes them more desirable since it results in density reduction. Several features in the properties of polyester make it hard to foam, such as its crystallinity, low melt viscosity and low melt strength [18, 37, 43, 49]. On the contrary, amorphous polymers such as Eastman's Easter copolyester and polystyrene have better rheological properties and therefore they are better foamed. The properties of the foam are determined by their cellular structure. The choice of a cell nucleator is important. The size, shape and distribution of cells in the foam are dependent on the type, size and distribution of the nucleator. In addition to the above, the blowing agent gas is another crucial selection, its solubility and diffusivity in the resin may greatly influence the final properties [31, 36, 44, 49, 50, 59].

2.2.3 Theory of Nucleation

Nucleation of microcells in polymer matrices involves several mechanisms. First, homogeneous nucleation that may occur in the homogeneous polymer. Second, heterogeneous nucleation that may occur at the interface. The third mechanism may be a combination of the first two [4, 44, 48]. It was found that the process of homogeneous nucleation could be described by [4, 33, 37, 39, 41, 48, 51]:

$$\Delta G_{\text{hom}} = -V_b \Delta P + A_{bp} \gamma_{bp} \tag{2.1}$$

where ΔG_{hom} is the Gibbs free energy for homogeneous nucleation, V_b is the volume of the cell nucleus, ΔP is the pressure change, A_{bp} is the surface area of the microcell nucleus, and γ_{bp} is the surface energy of the interface. However, if the microcell is spherical, the process is described by [2-5]:

$$\Delta G_{\text{hom}} = -\frac{4}{3}\Pi r^3 \Delta P + 4\Pi r^2 \gamma_{bp} \tag{2.2}$$

The critical radius for which $\frac{dG}{dr} = 0$ is $r^* = \frac{2\gamma_{bp}}{\Delta P}$ (2.3)

Therefore,

$$\Delta G^*_{\text{hom}} = \frac{16\Pi}{3\Delta P^2}\gamma^3_{bp} \tag{2.4}$$

The activation energy for cell nucleation is [4,6]:

$$\Delta E^*_{\text{hom}} = \Delta G^*_{\text{hom}} - \Delta U \tag{2.5}$$

where ΔU is the change in potential energy between the polymer molecules.

$$\Delta U = U(T, P) - U(T_\circ, P_\circ) \tag{2.6}$$

Where T is temperature and P is pressure (high foaming pressure in case of physical blowing agent or low pressure of the gas released in the case of decomposition of chemical blowing agent).

$$U(R) = - \frac{U_{min} R^{12}{}_{min}}{R^{12}} + \frac{2U_{min} R^{6}{}_{min}}{R^{6}} \quad (2.7)$$

where U (R) is the potential energy, R is the distance between two polymer chains, and U_{min} is the potential energy at the equilibrium intermolecular distance R_{min}.

Therefore, the homogeneous nucleation rate can be determined by [4]:

$$N_{hom} = N_{\circ} \exp\left(\frac{-\Delta E^{*}_{hom}}{KT}\right) \quad (2.8)$$

where K is the Boltzmann constant, $N_{\circ}$ is a constant, which depends on the gas concentration and the frequency factor of nucleation.

In the case of a heterogeneous nucleation process, the rate of heterogeneous nucleation can be determined by [5,36]:

$$N_{het} = N_1 \exp\left(\frac{-\Delta G^{*}_{het}}{KT}\right) \quad (2.9)$$

Finally, for the combined mode, the rate of nucleation can be determined by [4]:

$$N = N_{het} + \omega N_{hom} \quad (2.10)$$

where ω is a reduction factor to N_{hom} due to N_{het}.

2.2.4 Blowing Agents

Blowing agents are classified into two classes, physical and chemical.

2.2.4.1 Foaming with Physical Blowing Agents

A physical blowing agent is either a gas or a liquid. In the case of a gas, high pressures are usually required in order to increase the kinetic energy of the molecules and therefore the solubility and the diffusion of the gas into the liquid polymer. In the case of liquid, the polymer is heated until the boiling point of the blowing agent, where its vaporization occurs. Releasing the pressure or boiling generates microcells. This step is initiated just before the gel time of the polymer when the polymer has been saturated with the gas [4, 39, 48]. Figure 2.2 shows a schematic for the foaming apparatus used to foam composites using nitrogen gas as a physical blowing agent [1].

Several factors need to be considered when selecting a physical blowing agent. The presence of the blowing agent should not affect the properties of the polymer resin nor influence the ability of the polymer resin to wet the fibers. Blowing agents should not have negative impact on the environment. For example, chlorofluocarbons and hydrocarbons have not been considered as blowing agents due to their negative environmental effects, even though they have been successful blowing agents [1, 2-5,39-47]. Nitrogen gas is a good example of a physical blowing agent since it is inexpensive and environmentally friendly.

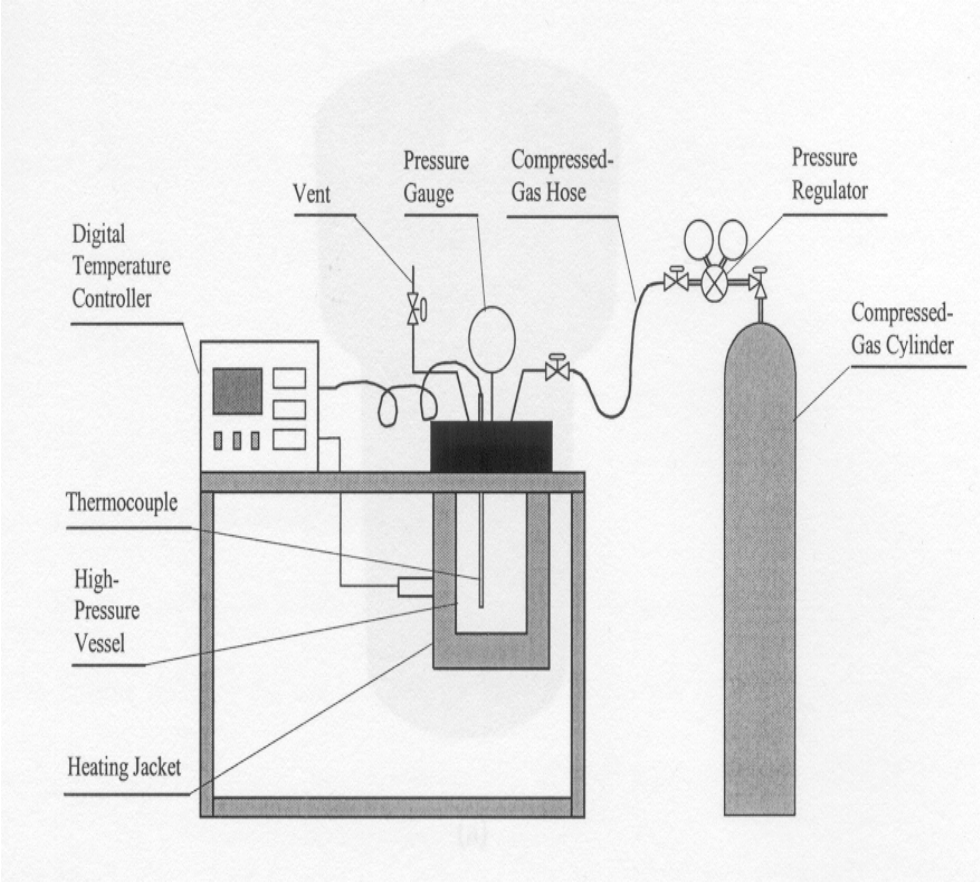

Figure 2.2 Schematic for the Foaming Apparatus Using Nitrogen Gas as Physical Blowing Agent [1]

The mechanism of cell growth is entirely different in the case of foaming with a physical blowing agent than in the case of foaming with a chemical blowing agent. Cell growth is controlled by the degree of saturation, rate of gas diffusion into the cells, pressure applied to the polymer matrix, the interfacial energy, and the viscoelastic properties of the polymer. Saturation times should be minimized to achieve an appropriate and uniform gas concentration. The foaming temperature can not be used to control the cell size of all amorphous polymers. However, the foaming temperature should be selected at a value near the glass transition temperature, while the saturation pressure should be selected to satisfy the required cell nucleation density. Both the saturation time and foaming time may be manipulated to achieve the required solution formation and cell growth requirements [1,2-5,40-45, 48].

Xu [1] found that at a constant temperature of 40°C, there is difference between the foam structures generated from pressures of 12 MPa and below, compared to those generated at pressures of 27.5 MPa and above. At constant saturation pressure of 34.4 MPa, with increasing temperature, cell size increases and cell density decreases.

The critical step in the process of production of microcellular polymers is the promotion of high cell nucleator rates in a polymer matrix [1]. The solubility of the gas at equilibrium state decreases as the pressure decreases and the temperature increases [4]. In the case of microcellular plastics, the cell sizes produced were in the range of 0.1 to 10 μm, the cell densities produced were in

the range of 10^9 and 10^{15} cells/cm^3, and specific density reduction in the range of 5% to 95%.

Semicrystalline polymers are relatively difficult to process to form microcellular structures compared to amorphous polymers. Therefore, there are significant differences between the processing of amorphous and semicrystalline polymers. The resulting foams may be considered amorphous if they have less than 10% crystallinity, which may be measured by various methods including Differential Scanning Calorimetry (DSC) [30, 39].

2.2.4.2 Foaming with Chemical Blowing Agents

Chemical blowing agents may be in the forms of a solid, and sometimes a liquid. The form of the blowing agent is taken in to consideration, as it must be compatible with the materials used. Sometimes, a mixture of different blowing agents is used to optimize the properties of the foam. Foaming is initiated once the blowing agent decomposes, releasing a gas, which spreads out across the structure nucleating microcells. Possible residuals may be retained in the structure. Foaming must be initiated just before the gel point of the polymer [22, 36-43].

Chemical blowing agents require only atmospheric pressure. For example, polyvinyl chloride plastisol may be foamed, in a typical atmospheric pressure using a chemical blowing agent such as azodicarbonamide [20-22]. Plastisol is coated on a substrate and transported through an oven heated to 200°C until the expansion of the foam occurs when the blowing agent reaches its decomposition temperature while the plastisol undergoes the gelation process [52]. The

formation of the foam is influenced by certain parameters, such as the gelation rate, the rheological properties of the gel plastisol, the rate of gas formation during the gelation process and the rate of the heat transfer during the formation of the plastisol. It is a challenge to match the decomposition temperature of the blowing agent and the gelation [52].

Another example where the foaming process using a chemical blowing agent is applied is in the case of plastics. The processing pressure in rotomolding, where plastics are foamed, is not high, which restricts use of physical blowing agents. Therefore, a chemical blowing agent should be used for developing foam structures in rotomolding. The selection of an appropriate blowing agent is crucial in the process of foaming plastics since the final foam structure is influenced by the characteristics of the chemical blowing agent. In order to be able to form a foamed structure in plastics using a chemical blowing agent, the decomposition temperature of the blowing agent, should be higher than the melting temperature of the polymer matrix [19].

The cell growth mechanism of foaming with a chemical blowing agent is different from that of foaming with a physical blowing agent. The usage of a chemical blowing agent requires only atmospheric pressure. Therefore, when the blowing agent decomposes and releases gas, the amount of gas that dissolves in the polymer is negligible due to the low pressure applied. When the cells are nucleated through the decomposition of the blowing agent, the pressure in the nucleated cells will be increased while the environmental pressure of the polymer matrix will remain the same. This is due to the continually generated gas [16, 22].

Chemical blowing agents are generally used when a low percentage of density reduction is desired. However, the density may be controlled by altering the concentration of the blowing agent. The higher the concentration of the blowing agent, the lower the density since more gas would be released [19].

Cell coalescence is an important phenomenon, which should be considered in the foaming process. When the cells are generated, adjacent cells may be in contact according to the laws of thermodynamics. Adjacent cells tend to coalesce due to lowering of the free energy by the reduction of the surface area of the cells [2, 19-22].

Cell coarsening is another important phenomenon, which should be considered in the foaming process. When two adjacent cells are of different size, the gas will diffuse from the smaller cell to the larger one due to the pressure difference in each cell. As a consequence, the smaller cell will continuously get smaller and on the other hand, the larger cell tends to get larger, which will eventually results in merging of both cells into one big cell [2, 20, 21, 39-42].

Therefore, when cell coarsening occurs, the cell population density deteriorates and consequently, the mechanical properties also deteriorate. Efforts were made to establish effective strategies for minimizing cell coarsence, which may be achieved by producing a fine cell foam structure in rotomolding [2, 21, 39-42].

If any air pockets are trapped in the polymer melt, huge cells are developed in the cellular structure since air pockets behave as nucleating sites for foaming and they prevent the formation of small cells (due to cell coarsening).

Therefore, the size of these pockets should be minimized, to form a fine cell structure.

To conclude this discussion, careful attention must be paid when selecting the chemical blowing agent. Several critical parameters are involved which may include the decomposition temperature, the decomposition rate, and the amount of gas generated.

2.2.4.3 Comparison Between Chemical Blowing Agents and Physical Blowing Agents

The key factors to introduce and commercialize a new process in industry are the productivity rate and the cost of the process. If these two factors were reasonable, the industry would probably be attracted to the process and investigate the possibility of applying it. If the new process was capable of producing a product with acceptable properties and at least the same quality of the current process, then it is likely to be adopted by the industry.

Considering the foaming process using the physical blowing agent, the first thing to notice is the total time needed for the process. Xu et al [1] found that the overall time needed for foaming, using the physical blowing agent, is almost twenty hours (30 minutes for sample preparation, one hour to secure the pressure vessel, twelve hours for saturation, three hours of curing, and four hours of post curing). This is considered one of the slowest processes, if not the slowest, used to fabricate composite structures. On the other hand, it would be very expensive to buy a huge pressure chamber to be able to produce larger quantities. Due to all the disadvantages of using the physical blowing agent in the foaming process, it is

almost impossible for the industry to apply it. The only advantages to using a physical blowing agent are that no residuals are retained in the structure and that it can be environmentally friendly since one has control over which gas to use.

On the contrary, considering the foaming process using the chemical blowing agent, several advantages would be noticed. First, the overall time of the process is minimum since the saturation cycle is eliminated. The process is also very simple and easy to apply. The materials needed are relatively cheap. No expensive equipment is needed to foam by a chemical blowing agent.

There are also several technical advantages for foaming via the chemical blowing agent, since one has control over the concentration of the blowing agent used which reflects the percentage of density reduction. Foaming via the chemical blowing agent provides flexibility as one has several blowing agents to choose from (which are usually cheap as well) and one may also use a mixture of blowing agents. Therefore, one may be able to manipulate the parameters, according to the required properties of the composite fabricated, and prepare extra material while still being able to use the same equipment.

In conclusion, the major advantages of foaming with a chemical blowing agent are the high productivity, the relatively low cost of production, the flexibility it provides, and the safety of using such a process. However, it is also worth mentioning that chemical blowing agents have a few negative features. The released gases such as carbon dioxide may not be environmentally friendly, and the residuals retained in the polymer may be harmful to the properties of the material.

2.3 Development of 3DCMC and their Properties

2.3.1 Development of 3DCMC

Gu et al [16] found that voids in 3D composites do not have a significant effect on the strength of the composites. The research was carried further by Carlson et al [13] who modified the epoxy matrix of 3D woven composites by the inclusion of hollow glass microspheres into the matrix. The purpose was to reduce the density. Density reduction of 13% was attained, and an increase in impact resistance was obtained. However, the trial was not successful since uniform distribution of the microspheres in the epoxy rich block was difficult to attain, in addition to other problems including the observed increase in the viscosity of epoxy resin. This may be due to the clustering of the microspheres near the surface of the composite [13].

Xu et al [1] decided to make use of the two studies of Gu and Carlson. They purposely introduced voids in 3D composites. They used a phenomenon, which is observed several times in our daily life. They decided to foam the epoxy matrix, thus purposely remove the matrix resin and spread microcells across the composite structure.

Xu et al [1] found that foaming the epoxy matrix of 3D woven composite by nitrogen gas as physical blowing agent successfully attained uniform distribution of the microcells in the epoxy rich block [1]. Figure 2.3 [1] shows the uniform distribution of microcells present in epoxy resin EPON 9405 from Shell Chemical Company. The foaming time was two hours while the foaming pressure was 3.7 MPa.

Xu [1] applied saturation temperature of 40°C for approximately twelve hours in order to ensure a complete saturation of Nitrogen in epoxy. The epoxy resin was cured at 100°C. Xu [1] also found that the gel point can be reached after 25 minutes at 150°C.

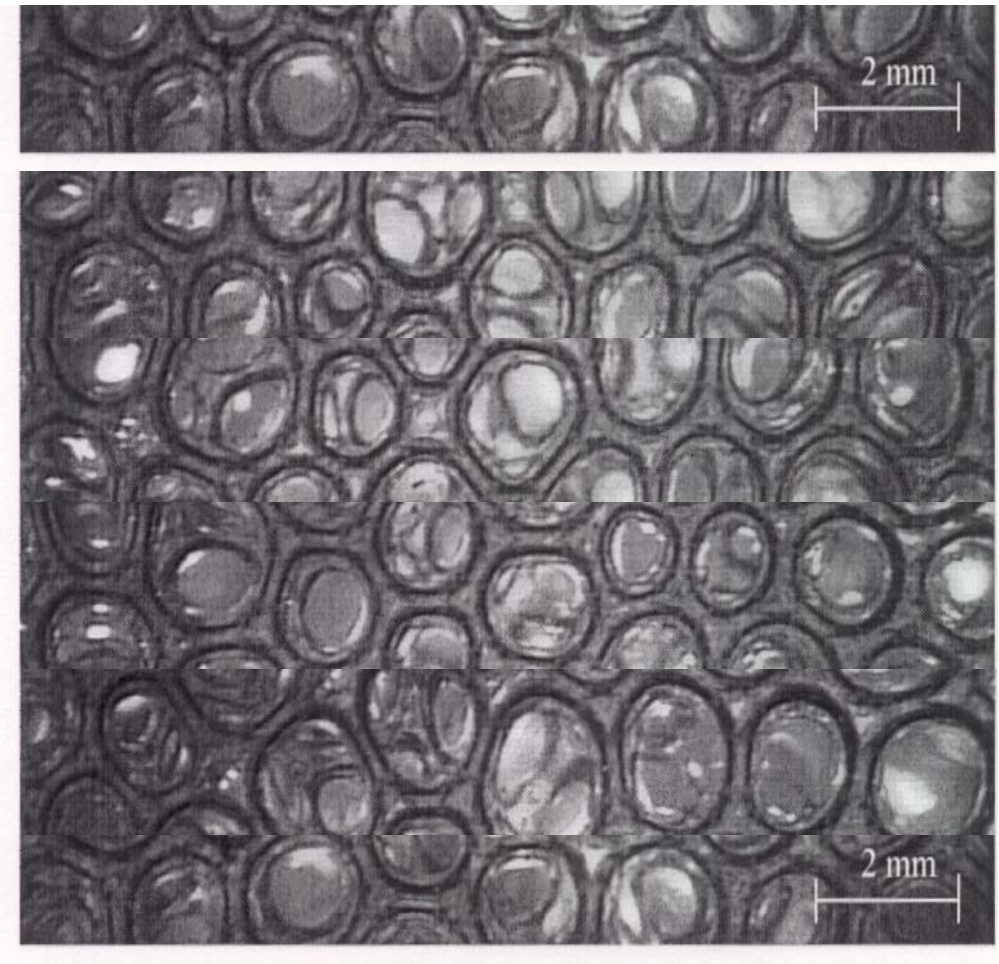

Figure 2.3 Distribution of Microcells Present in Epoxy Rich Block [1]

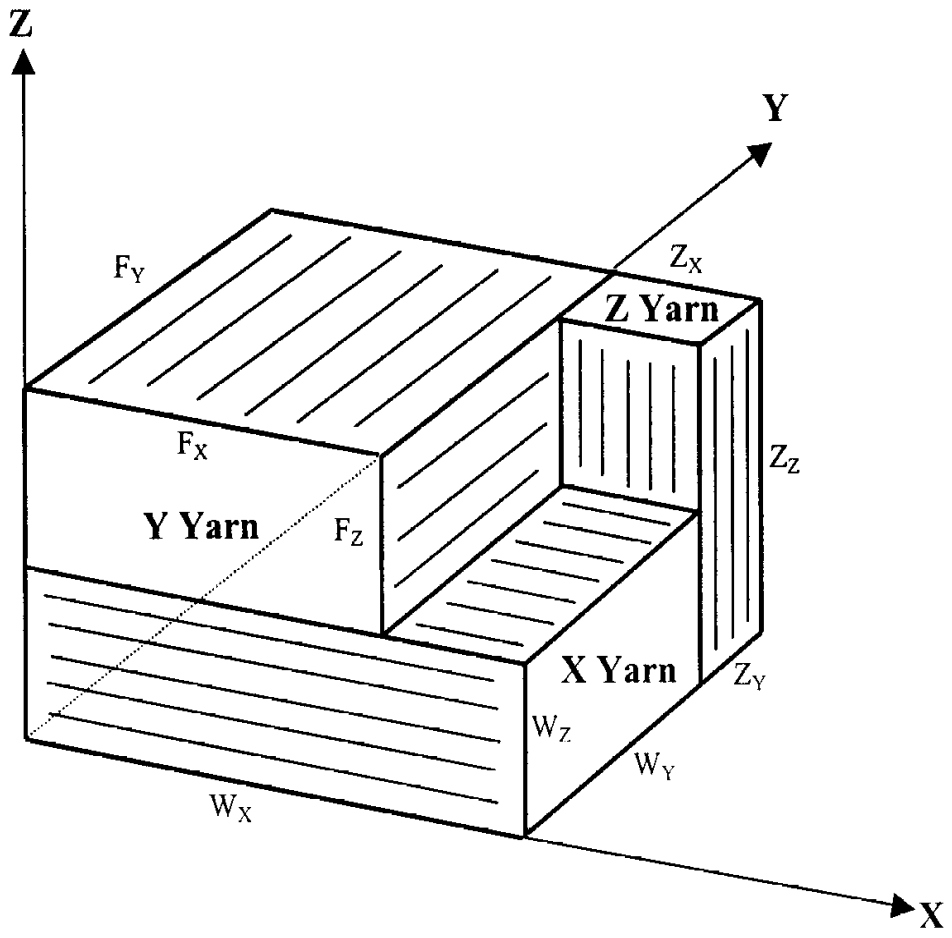

Figure 2.4 Schematic Diagram of an Internal Unit Cell of 3D Woven Fabric Composite [1]

2.3.2 Internal Structure and Geometry of 3DCMC

The internal structure consists of empty pockets, formed during the foaming process by blowing away epoxy resin from epoxy pockets, which otherwise are filled with epoxy resin, as in the case of 3DRMC [1].

Xu [1] observed cross sections of the composite samples. He found that epoxy resin in epoxy rich block was removed. Xu [1] found that 3DCMC had slightly lower fiber volume fraction than 3DRMC.

Xu [1] tested two samples of 3D composites with different fabric geometry and compared them to their corresponding 3DRMC. Xu [1] found that average density of 3DCMC was 28-37% less than 3DRMC.

Figure 2.4 shows the unit cell of a 3D woven composite [1]. There are two epoxy pockets. In the 3DRMC the pockets are usually filled with resin, while in the 3DCMC, the pockets are usually empty.

The net volume of the resin pocket can be calculated following equation 2.11:

$$\text{Net Volume of Resin} = 2\, X_d Y_d Z_d \qquad (2.11)$$

Where:

X_d is the side of the square in the X direction (assume square cross-section).

Y_d is the side of the square in the Y direction.

Z_d is the side of the square in the Z direction.

2.3.3 Mechanical Properties of 3DCMC

Xu compared the mechanical properties of 3DCMC and 3DRMC. He found that 3DCMC demonstrated similar ultimate tensile strength and elastic

modulus, lower flexural strength in bending but higher tangent modulus, and similar impact energy absorption at lower impact velocity. Tables 2.1 and 2.2 show the tensile strength and flexural strength under bending of both 3DCMC and 3DRMC. The TM and TMR represent 3DCMC while the TS and TSR represent 3DRMC.

Empty pockets and voids across the structure of 3DCMC are the reason for the large deformation during the impact. If microcells can spread out the epoxy resin and do not penetrate the yarns, optimum properties would be achieved for 3DCMC [1]. However, the loss in properties was negligible compared to the loss in density.

There was no data available for compression tests of 3DCMC. It is crucial that the compression resistance of 3DCMC be studied in the future as it is an important property of the structure.

Table 2.1 Tensile Strength of 3DCMC and 3DRMC [1]

Composite	Average Strength (10^6 Pa)	Standard Deviation (10^6 Pa)	Specific Strength (10^6 Pa-cm^3/g)	Standard Deviation (10^6 Pa-cm^3/g)	Thickness (mm)
TM	423	27.09	419.22	26.85	4.57
TMR	447.81 514.99	33.03 39.03	324.50 373.18	23.93 28.28	5.40 4.57
TS	549.06	48.19	510.28	44.79	4.50
TSR	506.21 591.86	40.42 48.50	366.82 428.89	29.29 35.14	5.40 4.50

Table 2.2 Flexural Strength in Bending of 3DCMC and 3DRMC [1]

Composite	Average Strength (10^6 Pa)	Standard Deviation (10^6 Pa)	Specific Strength (10^6 Pa-cm^3/g)	Standard Deviation (10^6 Pa-cm^3/g)	Thickness (mm)
TM	264.39	21.19	262.03	21.00	4.57
TMR	351.96 467.58	16.64 22.11	255.04 338.83	12.06 16.02	5.40 4.57
TS	302.36	21.11	281.01	19.62	4.50
TSR	418.13 580.73	50.39 69.99	302.99 420.82	36.52 50.72	5.40 4.50

3. EXPERIMENTAL PROCEDURES

3.1 Materials Used

- 3 D glass fabric, from 3 TEX, Inc. The properties of the fabric are listed in table 3.1.
- Epoxy resin, EPON 9405, from Shell Chemical Company.
- Curing Agent, ANCAMINE 9470, from Shell Chemical Company. The mix ratio was set by the manufacturer to be 100/28.
- Accelerator EPICURE 537, from Shell Chemical Company. Used only for 3DRMC and 3DCMC foamed by chemical blowing agent.
- Breather (Air weave N10 Bleeder), from AirTech International, Inc. Used for high pressure cures, 10 oz/yd^2. Used to imbibe excessive resin.
- Release Ply, from AirTech International, Inc. Tightly woven polyester fabric that offers high service temperature up to 204°C. Used to prevent the composite from sticking to the bleeder.

3.2 Fabrication of 3DCMC by a Physical Blowing Agent

The glass fabric was cut in dimensions of 5.5'' x 8.5'' and the resin material used was 50 grams, then 14 grams of the curing agent (28% of the resin's mass) were added. The fabric was completely wet by the mixture of resin and curing agent and well vacuumed in an oven to ensure that the resin entirely wet the preform. The system was placed in the pressure vessel and carefully secured in preparation for high pressures and temperatures. A great detail of the equipment and method is available in the dissertation of Xu [1].

Table 3.1 Properties of the 3D Woven Glass Fabric Used to Fabricate All the Composite [59]

Property	Value
Product	100% E-glass roving
Mass/Unit Area	104 oz/yd^2
Insertions/Length	4.38 Insertions/inch
Number of Ends	5 ends/inch
Number of Layers X Direction	3
Number of Layers Y Direction	4
Linear Density of Warp End	2.4 x 10^3 tex
Linear Density of Warp Yarn for Internal Layer	3.6 x 10^3 tex
Linear Density of Fill Yarn for Internal Layers	1.2 x 10^3 tex
Linear Density of Fill Yarn for Top Layer	1.2 x 10^3 tex
Linear Density of Fill Yarn for Bottom Layer	1.2 x 10^3 tex
Linear Density of Z Yarn	276 tex
Fiber Weight Fraction (Warp)	49.6 %
Fiber Weight Fraction (Filling)	49.657%
Fiber Weight Fraction (Z Yarn)	0.743%

The system's pressure was set and maintained at 3 MPa for all the tests. Five samples were fabricated under five different conditions. The saturation times were 12 hours at 40°C, 8 hours at 40°C, 4 hours at 40°C, 2 hours at 40°C, and 2 hours at 60°C.

After the saturation time passed, the system's temperature was increased to the curing temperature. The curing time was three hours at 100°C for the first four tests, and two hours at 100°C, for the last test.

It was noticed that, once the temperature was raised to the curing temperature, the system's pressure gradually increased as well. This can be explained by the ideal law of gases PV = nRT.

At the end of the curing period, the pressure was released, and cells were generated. The system's temperature was maintained at the curing temperature for additional four hours for the first three tests, and two hours for the last two tests. The sample assembly was taken out of the vessel at the end of the process. A sample from each condition was well polished and analyzed under the microscope.

3.3 Fabrication of 3DRMC

The 3D glass fabric was cut in the dimensions of 8'' x 5" and its mass was documented. The EPON 9405 was weighed such that its mass was equal to the mass of the fabric then the curing agent was added following the ratio of 100/28. The last item added to the mixture was the accelerator, with a concentration of 2.1% of the total weight of resin and curing agent. The mixture was stirred for one minute.

The resin was applied to wet the entire preform before it was placed in the mold. The mold with the preform was placed in a vacuum oven to remove any air bubbles trapped in the structure. The temperature, at this stage was 100°C. The system was then placed in the oven at a temperature of 150°C for two hours, to ensure stabilization of the matrix properties. At the end of the two hours, the system was taken out of the oven and 3DRMC was fabricated.

3.4 Fabrication of 3DCMC by a Chemical Blowing Agent

3.4.1 TGA of the Chemical Blowing Agents

TGA experiments were applied to study the decomposition behavior of the selected blowing agents. The model of the equipment used was Pyris 1, from PERKIN ELMER. The maximum temperature which can be applied on the equipment was 1000°C, while the maximum weight was 50 milligrams.

Several blowing agents were selected, for example, citric acid, sodium sulfate, and sodium bicarbonate. Each blowing agent was tested under 100°C and 150°C.

Twenty milligrams of the blowing agent were weighed and placed in the equipment under heat for several hours. The heating rate used was 75°C/minute for those tested under 100°C, and 125°C/min for those tested under 150°C.

3.4.2 Foaming Process

The procedure was the same as the method used to fabricate 3DRMC, except that there was sodium bicarbonate added in concentrations of 2.5%, 5.0%.

7.5%, 10.0 %, 12.5% and 25.0 %. Also, the vacuum of the preform took place at a temperature of 50°C to avoid partial decomposition of the sodium bicarbonate.

3.5 Ignition Test

Samples fabricated under each condition were subjected to a high temperature of 700°C and maintained for four hours. Epoxy resin was burned and evaporated. At the end of the four hours, only glass fabric was retained unaffected. The mass of the fabric was reported in grams.

3.6 Four Point Bending Test

The four point bending was performed according to ASTM D6072 [26], on Instron model 5500R and load cell capacity of 4538 N. Figure 3.2 shows a schematic diagram of the four point bending fixture. The samples were all cut in the dimensions of 152 mm long and 25mm wide. The crosshead speed was 2 mm/min. The composites were deflected until rupture occurred in the outer fibers.

Four samples were tested, and the sample size was five for each. The first two samples compare the 3DCMC and 3DRMC in filling direction, and the last two samples compared the 3DCMC and 3DRMC in warp direction. Flexural strength and tangent modulus were calculated as shown in Appendix B.1 and B.2.

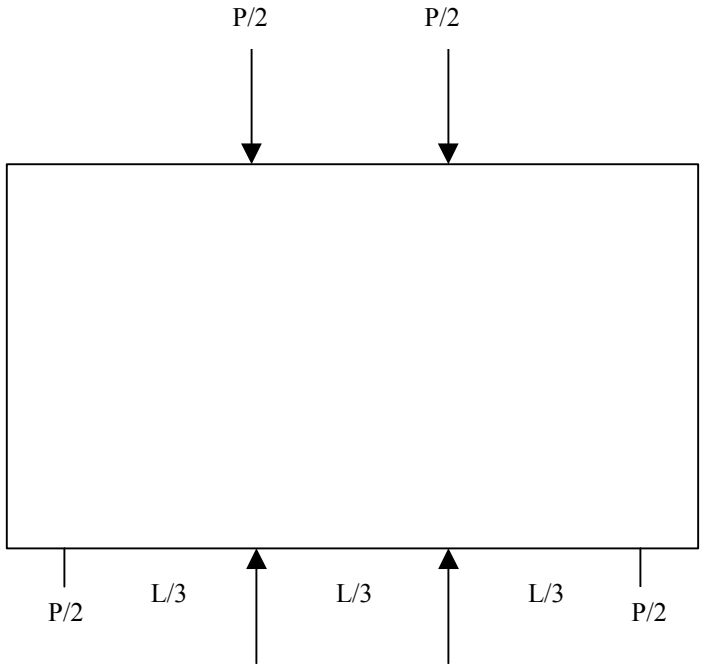

Figure 3.1 Schematic Diagram of the Fixture of Four Point Bending Test

3.7 Tensile Test

Each sample had a strain gage placed in the axial direction. One sample from each group had a strain gage placed in the transverse direction as well, to allow the calculation of Poisson's ratio. For the application of the strain gages, the procedure from the Vishay Student Manual for Strain Gages Technology sections 4.0-6.0 were followed using the three wire circuit [32].

The tensile test took place following the ASTM standard test method D3039/D3030M-00 [25]. The number of samples and sample size were the same as four point bending. The specimens were 152 mm x 25 mm. The tests were conducted on the Instron machine model 5500R with maximum load cell of 20KN.

The crosshead speed was 2 mm/min and the gage length was 100 mm. Tensile strength and tensile modulus were then calculated as described in Appendix C.

3.8 Impact Test

Drop weight tests were conducted on 3DRMC and 3DCMC. Two specimens from each group were tested. The specimens were cut into squares 126 mm x 126 mm. The object used to drop the weight was cylindrical with a 19-mm diameter, and a spherical nose made of steel. The mass of the object was 5.5 kg. The impact velocity was 3 m/s. The object had a sensor to detect its position. A detailed description of the equipment and the test method is described by Flanagan [58].

4. RESULTS AND DISCUSSION

4.1 Foaming by a Physical Blowing Agent

The parameters involved in the process of foaming by a physical blowing agent are saturation time, saturation temperature, curing time, curing temperature and foaming pressure.

4.1.1 Effect of the Saturation Time

The first three conditions tested (saturation times of 12 hrs, 8 hrs, 4 hrs) were successful, i.e. the structure was foamed. These conditions were tested under saturation temperatures of 40°C. However, the fourth condition which was tested at two hours of saturation under 40°C, was not successful, (i.e. the gas dissolved and diffused into the liquid resin, and was not enough to generate microcells which can be recognized).

The higher the temperature and pressure, the faster the solubility and diffusion of gas into the liquid resin. This is due to the corresponding increase in the kinetic energy of the molecules and therefore, the increased diffusion of gas into the cells. Therefore, the fifth condition attempted to keep the saturation time to two hours, so the saturation temperature was increased to 60°C, which increased the pressure as well, since the system had a constant volume. The test was successful and the saturation time of two hours under an optimum temperature of 60°C successfully foamed the composite structure. It was not possible to investigate increasing the saturation temperature any further, since that would speed up the curing of the resin which might cause the resin to reach the gel point before the initiation of foaming. If foaming is initiated after the gel

point, microcells will not form due to the high viscosity of the resin, and the formation of cracks is possible.

4.1.2 Effect of the Curing Time

The curing time determined by Xu [1] was three hours at 100°C and four hours post curing at the same temperature. When the saturation temperature was increased to 60°C, the resin has partially cured. Therefore, the forth and fifth tests were tested under curing time of two hours at 100°C and post curing time of two hours at the same temperature. The last test was successfully foamed.

Therefore, successful foaming by applying nitrogen gas as physical blowing agent was achieved with the following parameters: Saturation time of two hours under 60°C, curing time of two hours under 100°C and post curing time of two hours at 100°C.

Figure 4.1 shows the cross-section of a 3DCMC fabricated under saturation time of 12 hours.

4.1.3 Density

For each of the four successful tests, (saturation times 12, 8, 4 and 2 hours), the overall density of the composite was calculated. Figure 4.2 shows the relationship between saturation time and density. The method of calculating the density is shown in Appendix A.1.

It was seen that the higher the saturation time, the lower the overall density of the composite. This may be explained by the amount of gas diffused into the polymer resin, i.e. the higher the saturation time, the higher the amount of

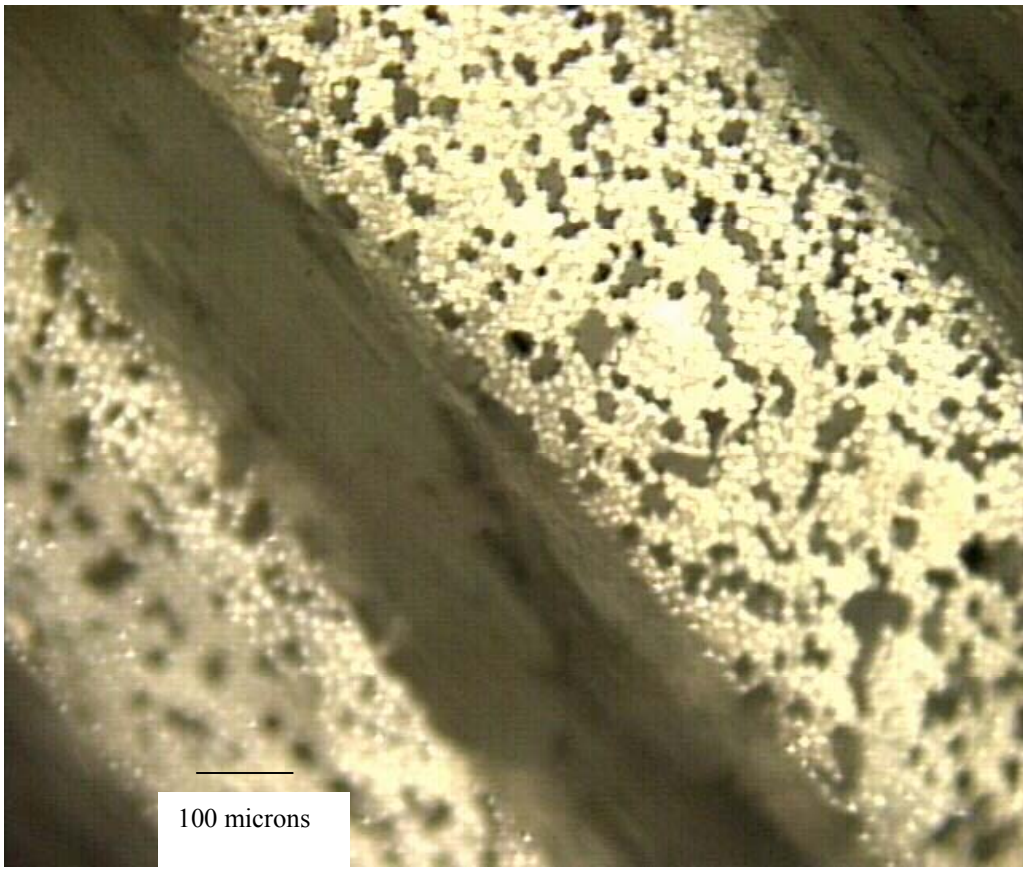

Figure 4.1 Cross-Section of a 3DCMC Fabricated under Saturation Time of Twelve Hours (100 x Magnification)

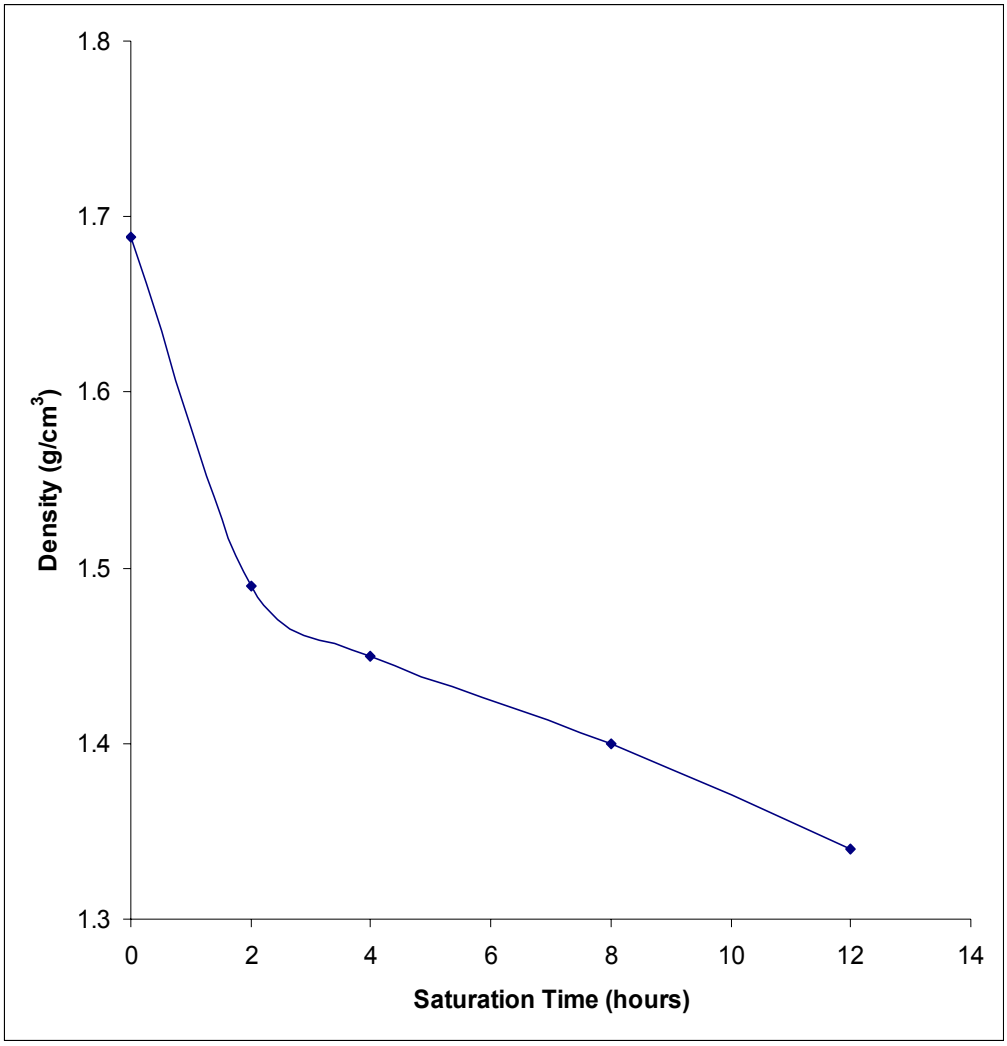

Figure 4.2 Saturation Time versus Overall Density of the Composite

gas dissolved into the resin, and hence, more microcells were generated when foaming occurs. Therefore, more resin is replaced with voids in the composite structure. This explains how increasing the saturation time reduced the density.

Density reduction of 11.73%, 14.1%, 17%, and 20.6% was achieved for 3DCMC fabricated under saturation times of 2, 4, 6 and 8 hours respectively. The density reduction was calculated following equation 4.1:

$$\text{DR } \% = \frac{\rho r - \rho c}{\rho r} \text{ x } 100 \tag{4.1}$$

Where ρ_r is the density of 3DRMC while ρ_c is the density of 3DCMC

4.1.4 Fiber Volume Fraction

The same samples used to calculate the density were used to calculate the fiber volume fraction in the composite. Figure 4.3 shows the relationship between saturation time and fiber volume fraction of the composites tested at 2, 4, 8 and 12 hours. As seen in figure, saturation time has no influence on the fiber volume fraction of the overall composite.

Theoretically, the total volume of the composite is a summation of the volumes of fibers, resin and voids. When foaming occurs under high pressure, the volume of the composite does not significantly change. After foaming is initiated, the volume of the resin is reduced at which time the volume of the voids start to increase, while the volume of the fibers is not expected to change. Therefore, the loss in the volume of resin is compensated by the gain in the volume of voids, i.e. the fiber volume fraction of the overall composite should remain almost the same, regardless of the foaming parameters.

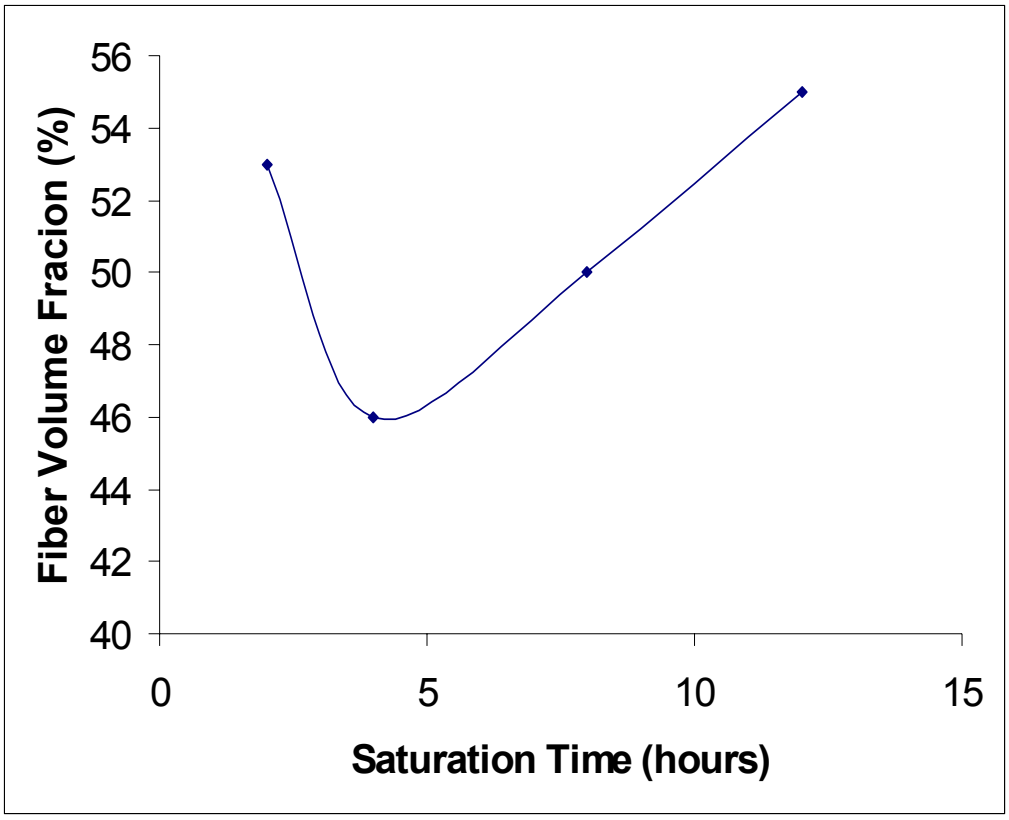

Figure 4.3 Saturation Time versus Fiber Volume Fraction of the Overall Composite

Only one sample for each condition was fabricated using the physical blowing agent. This was due to the fact that one test can investigate the possibility of successfully shortening the production time, which was the goal of this part of the study. Foaming by a physical blowing agent has many disadvantages, for example the high cost and danger of the equipment. Therefore, it was not of interest to further investigate the process of foaming by a physical blowing agent, since the search for an alternative method of foaming was the best solution to eliminate all the disadvantages associated with the process.

4.2 Foaming by Chemical Blowing Agent

A review of literature shows that foaming by a chemical blowing agent was successfully achieved in plastic structures. The method was investigated to be applied on composite structures.

The idea behind foaming by a chemical blowing agent is to mix an appropriate chemical compound and heat to the decomposition temperature, at which time gases are released initiating microcells in the structure.

The challenge was to apply a blowing agent whose decomposition temperature coincides with the curing temperature of the resin. Also, whose decomposition can occur right before the gel point of the resin, for the reasons previously discussed. The higher the curing temperature, the quicker the crosslinking reaction of the thermosetting resin, and therefore the faster the curing occurs. Xu et al [1] determined the gel point of EPON 9405 resin, under 100°C and 150°C. They found that at 100°C, the gel time is two hours, while at 150°C the gel time is 25 minutes. Therefore, our goal was to obtain a chemical blowing

agent, whose decomposition temperature is 150°C and can decompose just before 25 minutes at that temperature, since this would reduce the production time.

4.2.1 Selection of an Appropriate Blowing Agent

After a thorough review of literature, several blowing agents were considered and TGA was applied on each at temperatures of 100°C and 150°C to study their decomposition behavior. The selected blowing agents included citric acid, sodium sulfate and sodium bicarbonate. Figures 4.4-4.8 shows the relationship between time versus mass for some of the tested blowing agents.

In the case of citric acid and sodium sulfate, at 100°C and 150°C, the time needed for decomposition was greater than five hours (only 5% reduction in mass after heating for five hours), therefore, both citric acid and sodium sulfate can not be used to foam EPON 9405.

In the case of sodium bicarbonate at 100°C, decomposition was initiated after approximately 4.5 minutes, while at 150°C, decomposition was initiated after approximately two minutes. In this case, sodium bicarbonate first loses carbon dioxide and becomes sodium hydroxide then under further heating, water will evaporate leaving only sodium oxide.

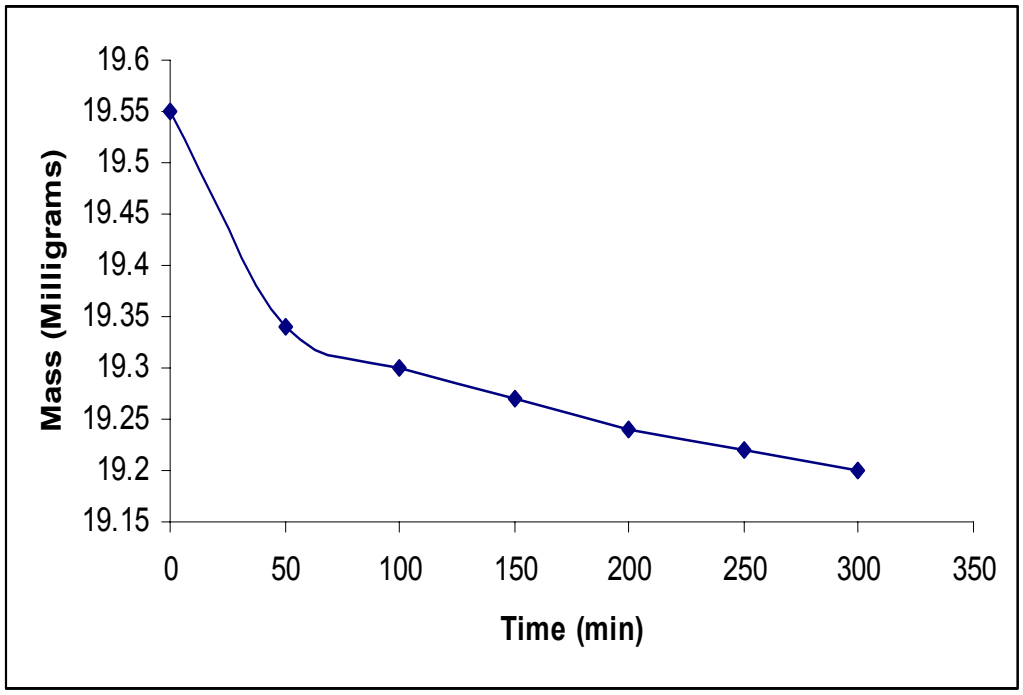

Figure 4.4 Time versus Mass of Citric Acid under 100℃

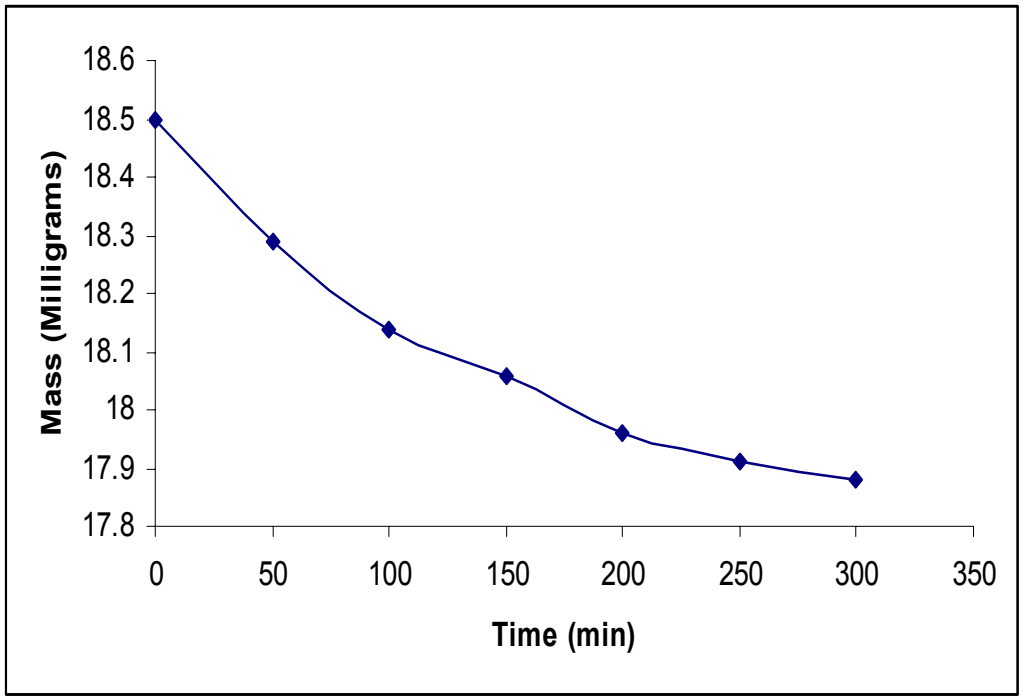

Figure 4.5 Time versus Mass of Citric Acid under 150℃

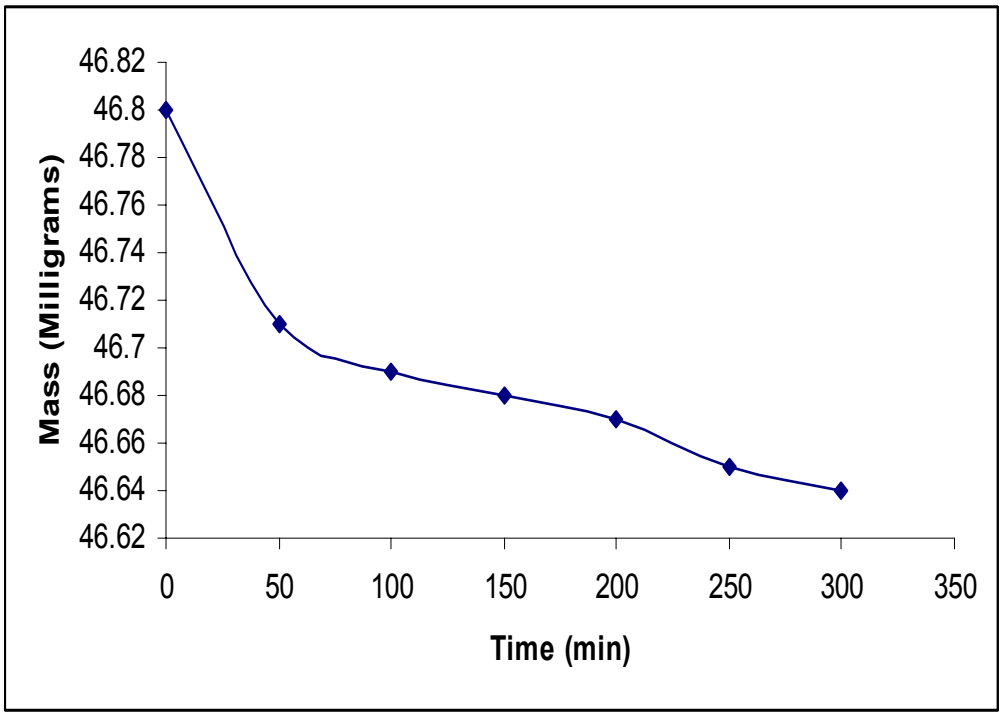

Figure 4.6 Time versus Mass of Sodium Sulfate under 100℃

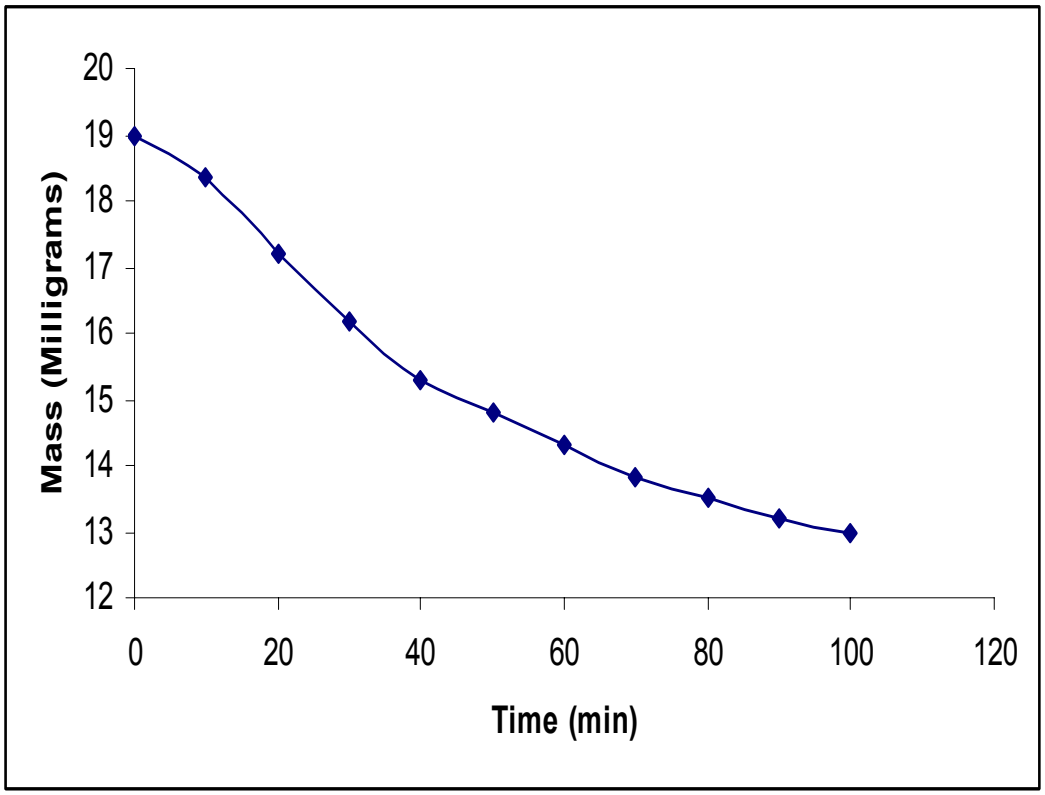

Figure 4.7 Time versus Mass of Sodium Bicarbonate at 100 ℃

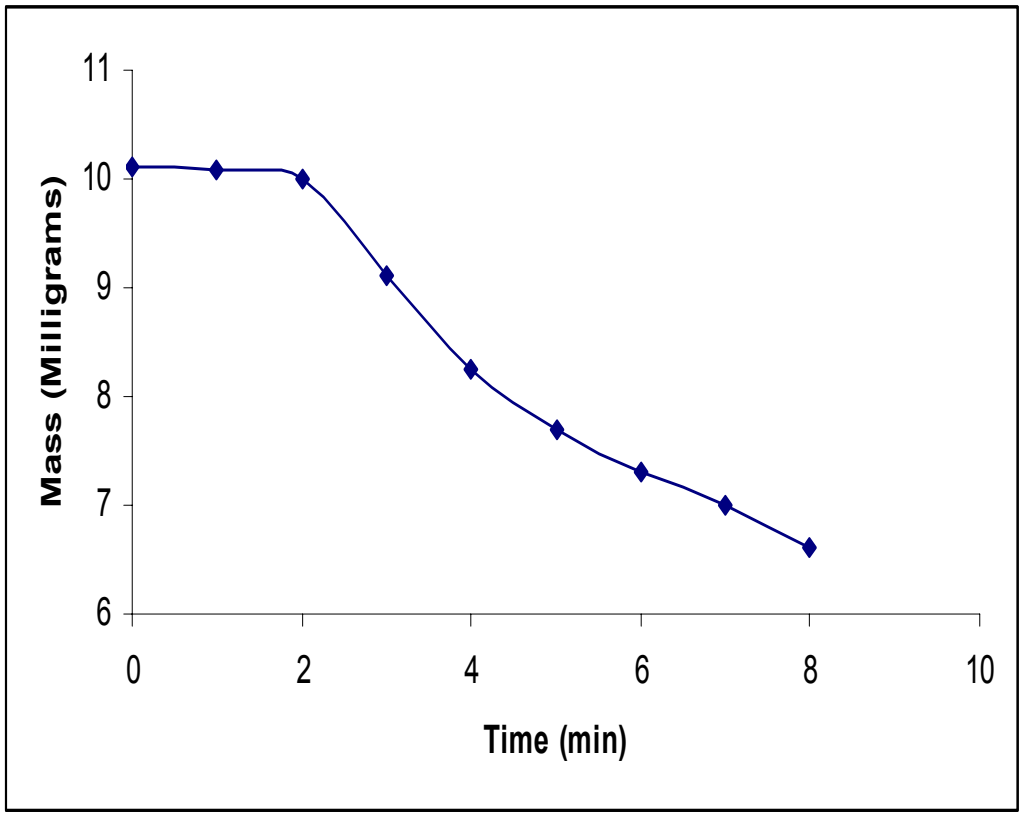

Figure 4.8 Time versus Mass of Sodium Bicarbonate under 150℃

Sodium bicarbonate was investigated further for possible use. Concentrations used in the literature range from 1% to 5% by weight. A pure resin test was conducted with 5% concentration of sodium bicarbonate at 100°C and at 150°C. The resin was not successfully foamed at either temperatures. The microcells were generated long before the gel time while the viscosity of the resin is too low to retain them.

The usage of an accelerator was investigated to shorten the gel time. Two percent of EPICURE 537 successfully reduced the gel time to approximately six minutes at 150°C. An experiment was conducted using the accelerator, and it was seen through the glass door of the oven that the resin foamed after approximately five or six minutes. The procedure was applied on composites and 3DCMC was successfully fabricated using sodium bicarbonate as a chemical blowing agent.

4.2.2 Density Analysis

Density control is crucial when considering 3DCMC. Xu et al [1] controlled density, when foaming by a physical blowing agent, by manipulating the foaming pressure. Density may also be controlled when using a chemical blowing agent and this can be done by manipulating the concentration of the blowing agent.

Six samples at different concentrations were tested to study their effect on the overall density of the composite. Concentrations of 2.5%, 5.0%, 7.5%, 10%, 12.5%, and 25% were applied. The sample size for each was five. Figure 4.9 shows the inverse relationship between the concentration of the blowing agent

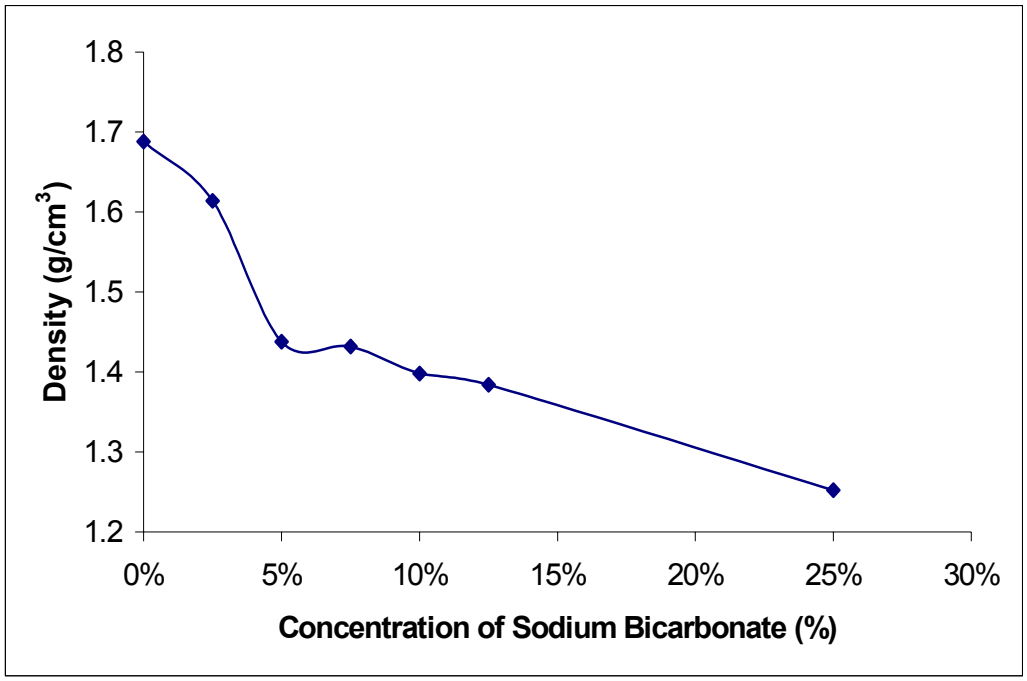

Figure 4.9 Concentration of Sodium Bicarbonate versus the Overall Density of Composites

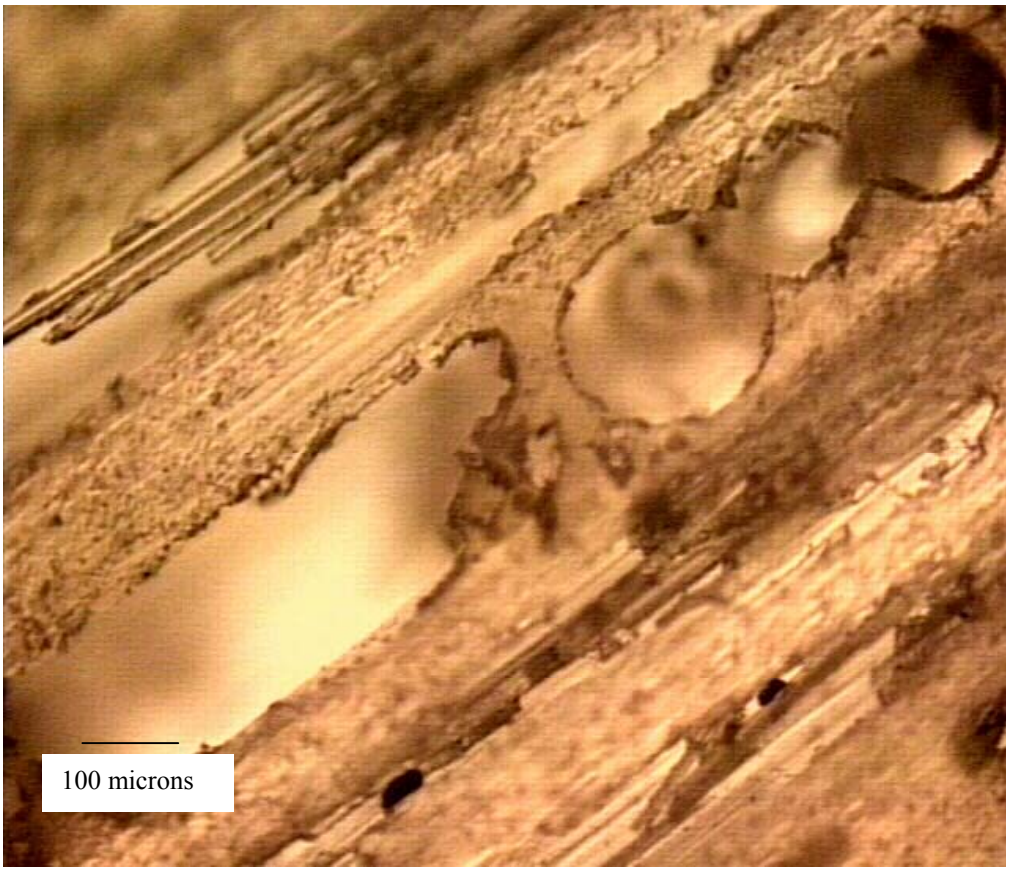

Figure 4.10 Microcells Present Across the Composite Structure Foamed by 5% of Sodium Bicarbonate (100 x Magnification)

and the overall density of the composite. This is due to the amount of gas released i.e. the higher the concentration of the blowing agent, the higher the amount of gas released, and therefore, the higher the amount of resin removed from the structure. Figure 4.10 shows part of the internal structure of 3DCMC foamed by 5% of sodium bicarbonate. Resin pockets were vacated, but microcells were present between the fibers in a yarn. This is a problem that remains to be solved, how can microcells be spread across the matrix material without penetrating the fibers? If this can be achieved, the strength of cellular composites will excel regular composites.

The density reduction was calculated by using equation 4.1. It was found that density reduction of 4.4%, 14.8 %, 15.1%, 17.1%, 18% and 25.8%, was achieved compared to 3DRMC, corresponding to concentrations of 2.5%, 5.0%, 7.5%, 10%, 12.5%, and 25%. Therefore, the density reduction was fast until 5% and then slower reduction when the concentration of sodium bicarbonate increases.

4.2.3 Fiber Volume Fraction Analysis

Fibers carry most of the load in the final composite, therefore, high fiber volume fraction will result in better strength and modulus in the composite. The concentration of sodium bicarbonate had great influence on the overall fiber volume fraction of the composite. The same six concentrations were tested and the fiber volume fraction for each was calculated.

The higher the concentration of sodium bicarbonate, the lower the fiber volume fraction. This is due to the increase in the total volume of the composite

when increasing the concentration of sodium bicarbonate. The tests were carried out with atmospheric pressure. Therefore, when foaming occurs, the volume of the resin increased, increasing the overall volume of the composite, since the pressure was negligible. Therefore, microcells were produced throughout the structure, decreasing the fiber volume fraction. For future work, it may be imperative to use the heat press to fabricate the composite. High pressures would resist the expansion of the volume. Therefore, when foaming occurs, excessive resin will be removed from the structure, while the total volume of the composite remains the same. The volume of the removed resin will be replaced with voids keeping the overall volume of the composite constant. It was found that the average fiber volume fraction was around 50%.

4.2.4 Mechanical Properties

It was proved that the higher the concentration of sodium bicarbonate, the higher the density reduction and the lower the fiber volume fraction. Therefore, an optimum concentration of 5% was selected to fabricate 3DCMC then test the mechanical properties of the fabricated composites and compare them to 3DRMC.

Four point bending test, tensile test, and drop weight impact test were conducted to compare the mechanical performance of 3DCMC and 3DRMC. Samples were cut to cover comparison in both warp and filling directions.

4.2.4.1 Bending Properties

The crosshead movement was constant throughout the test at 2 mm/min. The composites were deflected until repture occurred in the outer fibers. Figures 4.11-4.14 show typical load-deformation behavior for each sample. Flexural

strength and tangent modulus were calculated for each test. Table 4.1 shows the mean and standard deviation for flexural strength and specific flexural strength of 3DRMC and 3DCMC in both warp and filling direction. Table 4.2 shows the mean and standard deviation for tangent modulus and specific tangent modulus of 3DRMC and 3DCMC in both warp and filling direction.

For both filling and warp directions, the flexural strength of 3DRMC is approximately 10% higher than 3DCMC. Xu [1] found that flexural strength of 3DCMC foamed by physical blowing agent was 45% less than 3DRMC. This is due to the presence of microcells across the structure of the 3DCMC, which weakened the bonding between the matrix and the fibers. However, the specific flexural strength of 3DCMC was higher than 3DRMC, which proves that 3DCMC has better flexural strength/density than 3DRMC.

For both filling and warp directions, the tangent modulus and specific tangent modulus of 3DCMC were higher than 3DRMC. The tangent modulus was measured at the linear portion of the load-deformation curve. Therefore, it was measured way before rapture occurred. This means the voids across 3DCMC lowered only the failure load.

T-tests were performed to compare the flexural strength data and tangent modulus data of both 3DCMC and 3DRMC. P-values for each comparison are listed in table 4.3. It was concluded that with 95% confidence, there is no significant difference between data of 3DCMC and 3DRMC when comparing flexural strength and tangent modulus, in both filling and warp directions.

Table 4.1 Flexural Strength of 3DCMC and 3DRMC

Composite	Direction	Mean Thickness (mm)	Mean Flexural Strength (MPa)	Standard Deviation (MPa)	Specific Strength (MPa-cm^3/g)
Cellular	***Filling***	3.45	375.94	70.25	226.4699
Regular	***Filling***	3.7	413.63	99.91	211.0357
Cellular	***Warp***	2.65	266.66	69.86	160.6386
Regular	***Warp***	2.95	290.17	70.73	148.0459

Table 4.2 Tangent Modulus of 3DCMC and 3DRMC

Composite	Direction	Mean Thickness (mm)	Mean Tangent Modulus (GPa)	Standard Deviation (GPa)	Specific Modulus (GPa-cm^3/g)
Cellular	***Filling***	3.45	24.07	6.66	14.5
Regular	***Filling***	3.7	21.11	4.34	10.77
Cellular	***Warp***	2.65	11.52	3.72	6.93
Regular	***Warp***	2.95	9.21	2.05	4.69

Table 4.3 P-Values for each T Test Performed

Comparison	**Direction**	**P Value**
Flexural Strength	Filling	0.5
Flexural Strength	Warp	0.611
Tangent Modulus	Filling	0.43
Tangent Modulus	Warp	0.22

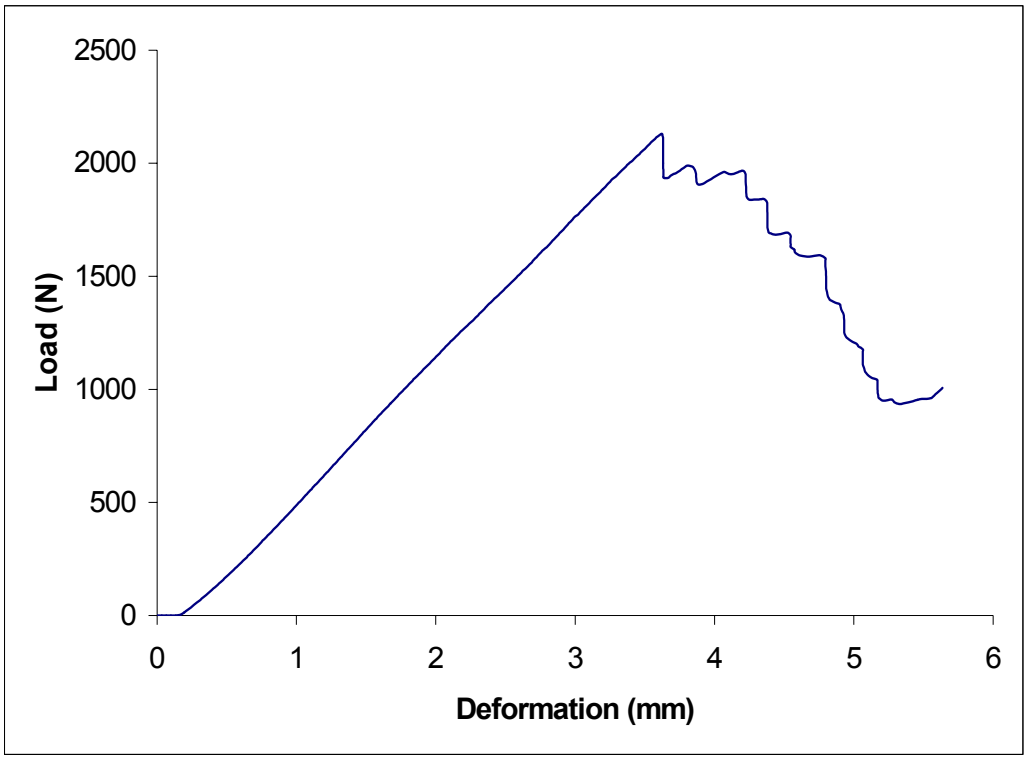

Figure 4.11 Selected Load-Deformation Curve for Cellular Matrix Composites (Filling Direction)

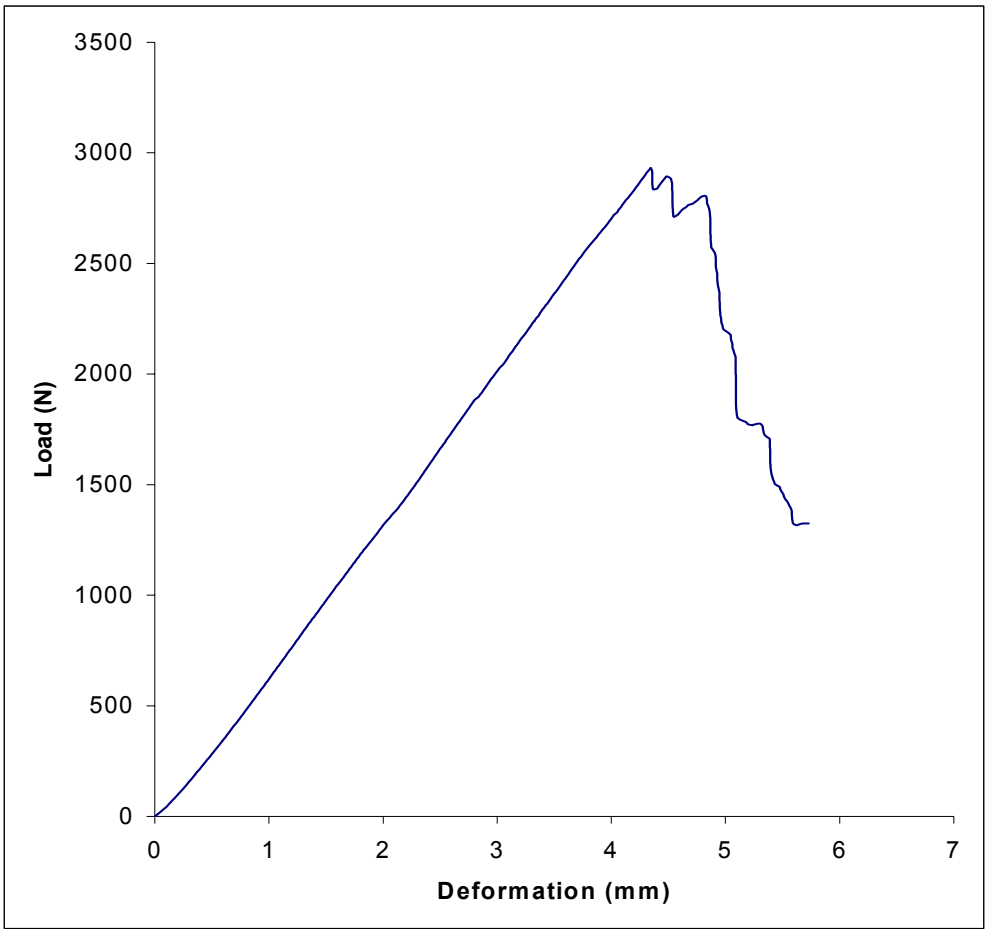

Figure 4.12 Selected Load-Deformation Curve for Regular Matrix Composites (Filling Direction)

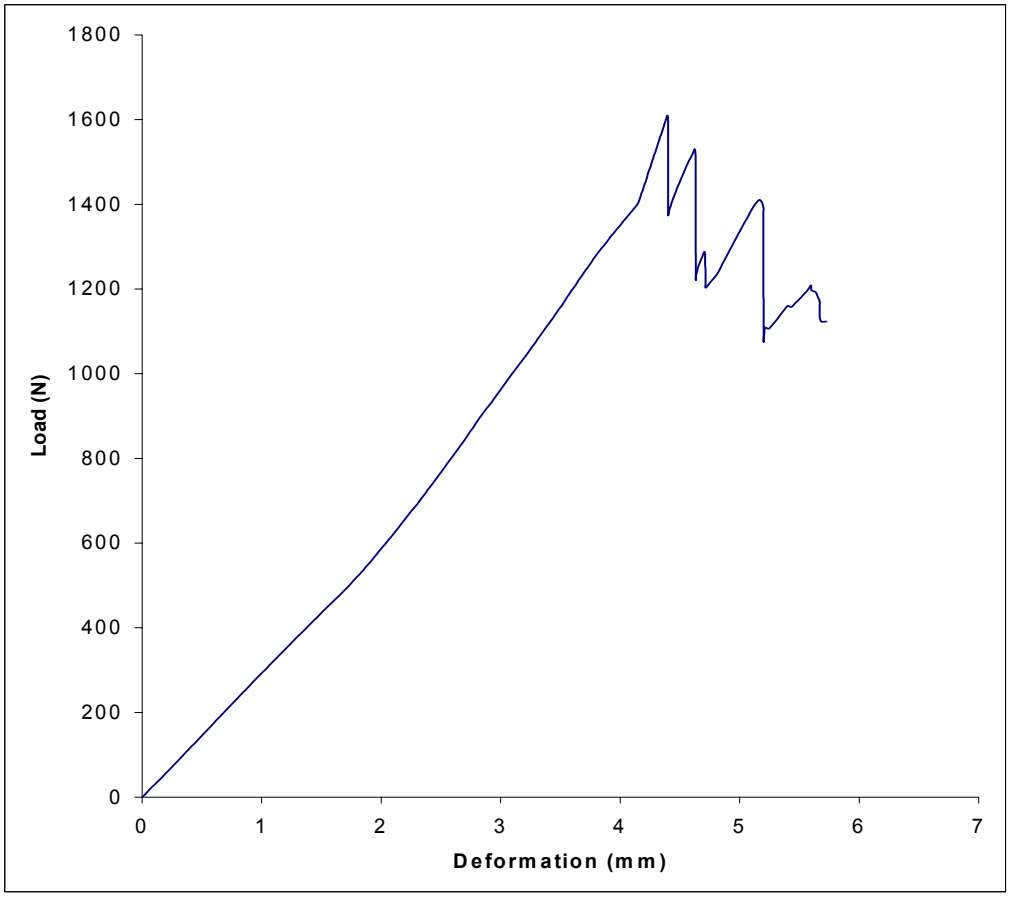

Figure 4.13 Selected Load-Deformation Curve for Cellular Matrix Composites (Warp Direction)

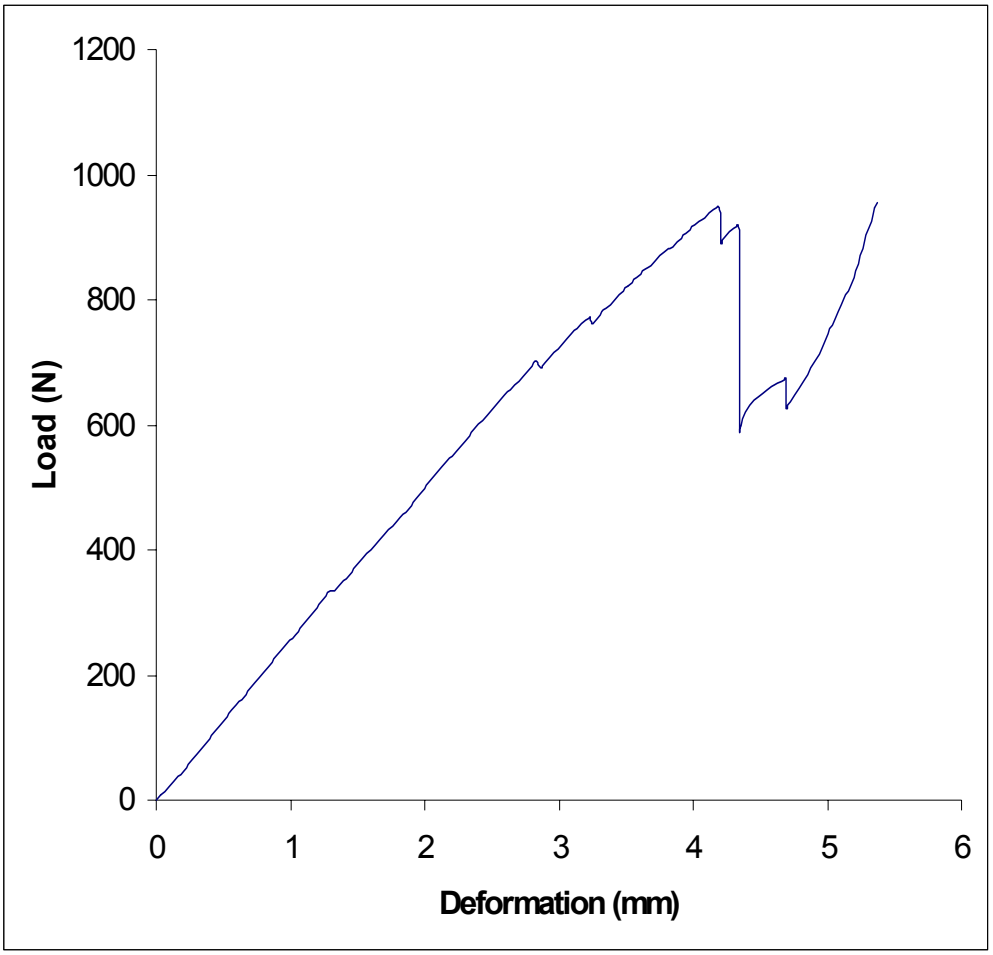

Figure 4.14 Selected Load-Deformation Curve for Regular Matrix Composites (Warp Direction)

4.2.4.2 Tensile Properties

For the case of filling direction, the tensile strength of 3DCMC was approximately 10% lower than 3DRMC. This is due to the presence of microcells across the structure of 3DCMC. However, the specific strength of 3DCMC was higher than that of 3DRMC. Accordingly, the tensile modulus of 3DRMC was higher than that of 3DCMC, while the specific tensile modulus of 3DCMC was higher than that of 3DRMC. This proves that 3DCMC has better strength and modulus/density. Therefore, it is worth trying to prevent the microcells from penetrating the yarns, and control their presence in the structure, such that they would only replace the resin in resin rich pockets.

For the case of warp direction, the same trend can be seen, the 3DRMC has similar strength and modulus as 3DCMC. However, the specific strength and modulus of 3DCMC is higher. Tables 4.4 and 4.5 show the strength and modulus data for 3DRMC and 3DCMC. Figures 4.15-4.18 show the linear portion of typical stress-strain curve for each case.

T-tests were performed to compare the tensile strength data and tensile modulus data of both 3DCMC and 3DRMC. P-values for each comparison are listed in table 4.6. It was concluded that with 95% confidence, there is no significant difference between 3DCMC and 3DRMC when comparing flexural strength and tangent modulus, in both filling and warp directions.

Table 4.4 Tensile Strength Data for 3DRMC and 3DCMC

Composite	Direction	Mean Thickness (mm)	Mean Tensile Strength (MPa)	Standard Deviation (MPa)	Specific Strength (MPa-cm^3/g)
Cellular	***Filling***	2.95	266.8	54.33	161.69
Regular	***Filling***	2.8	301	20.61	153.57
Cellular	***Warp***	2	212.2	62.83	128.6
Regular	***Warp***	2.1	196.4	22.81	100.2

Table 4.5 Tensile Modulus Data for 3DRMC and 3DCMC

Composite	Direction	Mean Thickness (mm)	Mean Tensile Modulus (GPa)	Standard Deviation (GPa)	Specific Modulus (GPa-cm^3/g)
Cellular	***Filling***	2.95	5.212	1.481	3.29
Regular	***Filling***	2.8	6.182	1.17	3.15
Cellular	***Warp***	2	3.382	0.433	2.05
Regular	***Warp***	2.1	3.83	0.2	1.95

Table 4.6 P-Values for each T Test Performed

Comparison	Direction	P Value
Tensile Strength	Filling	0.22
Tensile Strength	Warp	0.611
Tensile Modulus	Filling	0.28
Tensile Modulus	Warp	0.069

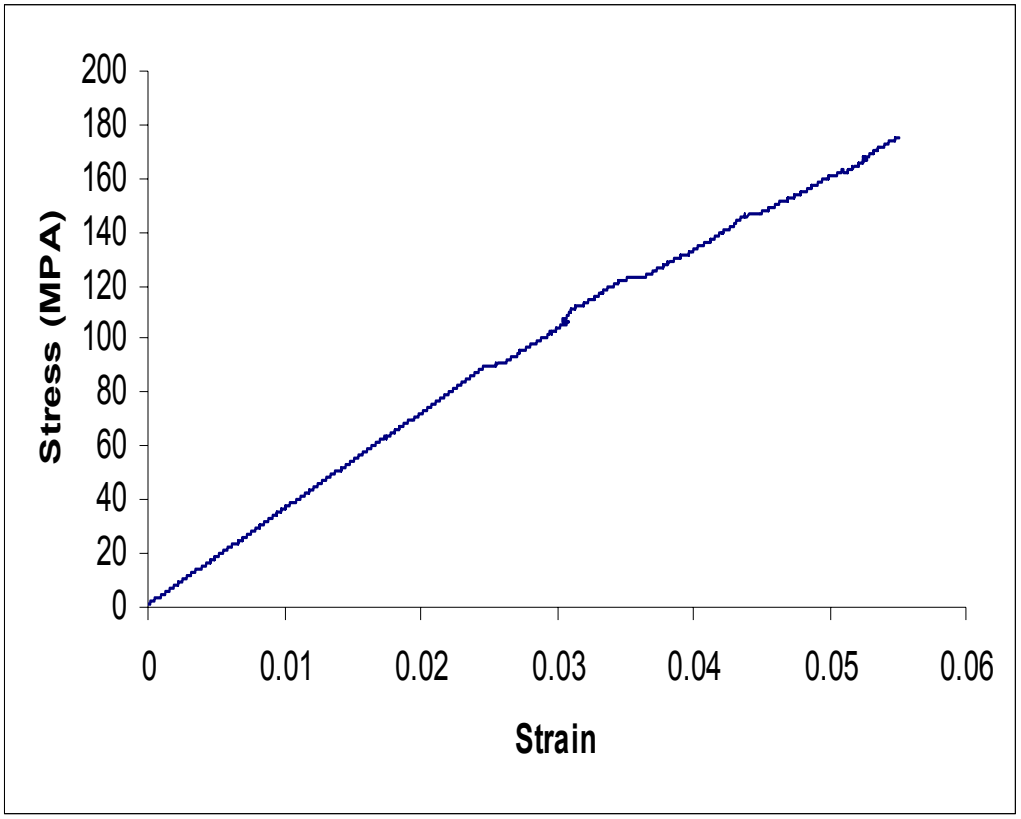

Figure 4.15 Linear Portion of Stress-Strain Curve of 3DCMC (Filling Direction)

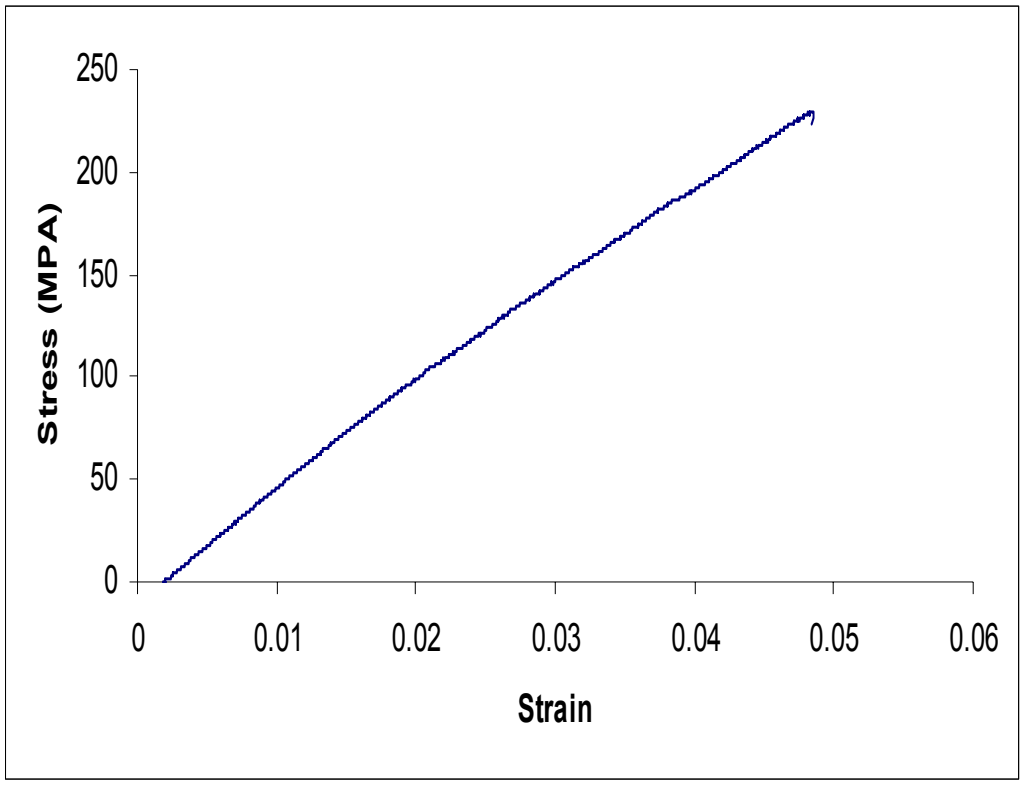

Figure 4.16 Linear Portion of Stress-Strain Curve of 3DRMC (Filling Direction)

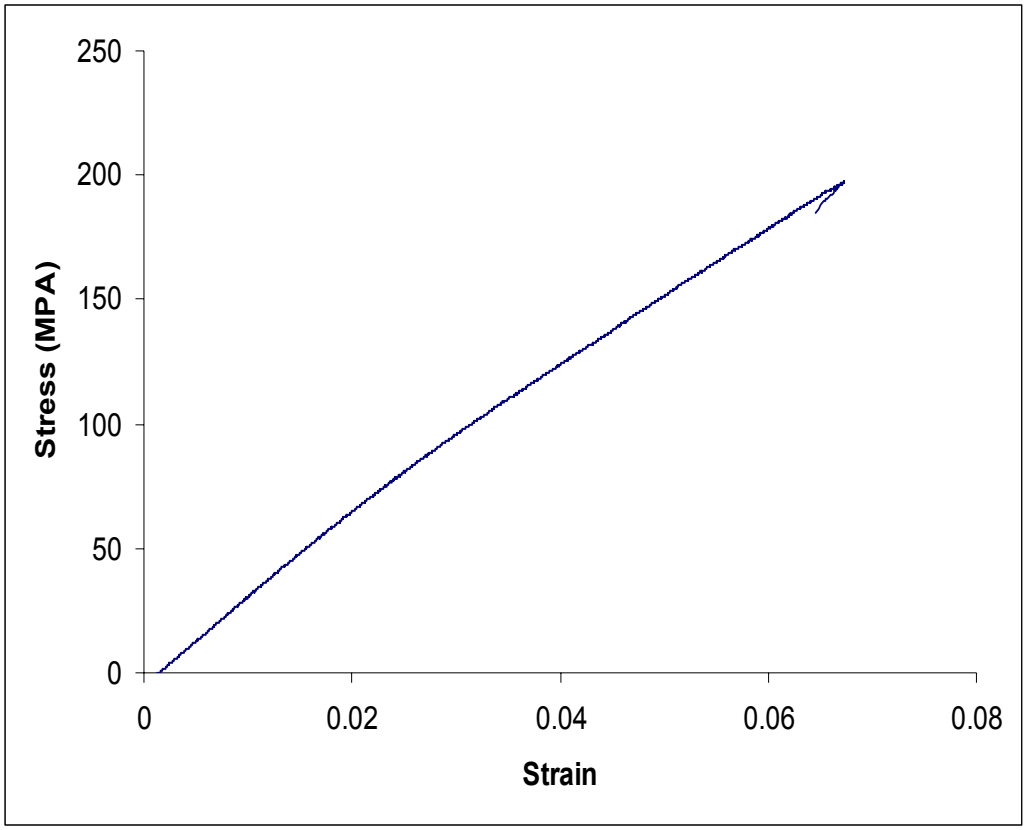

Figure 4.17 Linear Portion of Stress-Strain Curve of 3DCMC (Warp Direction)

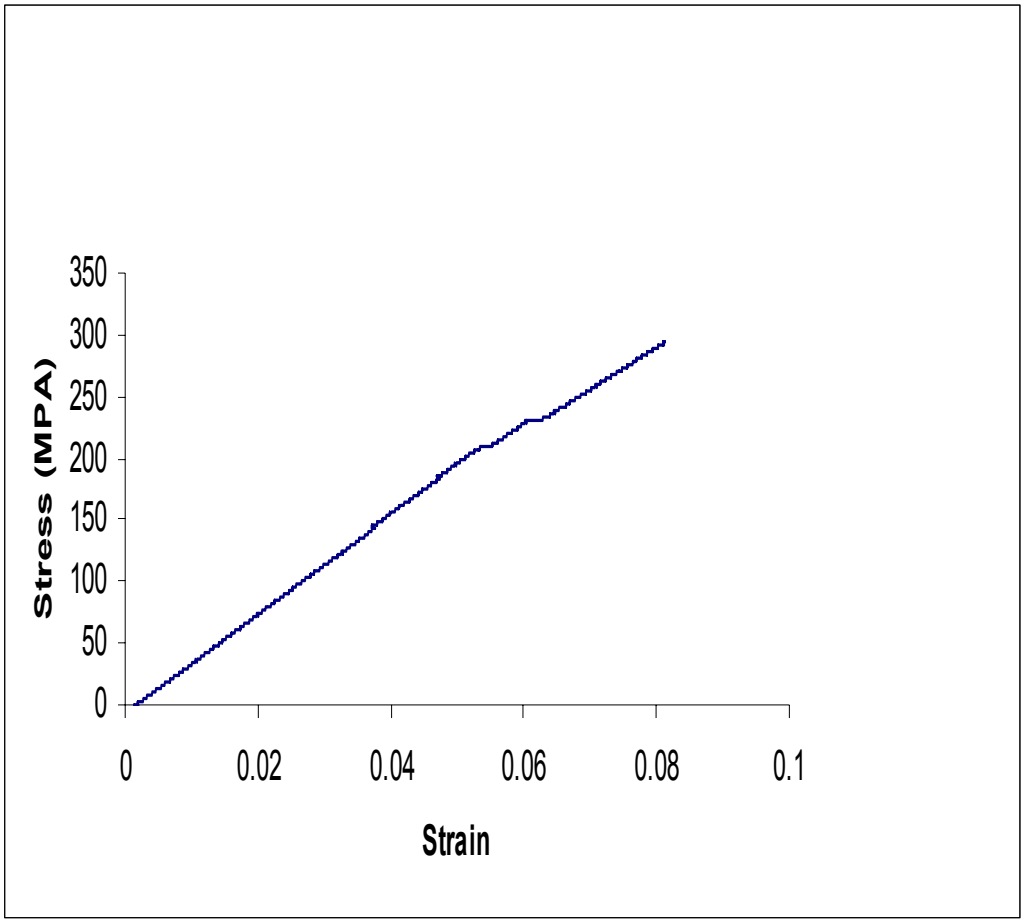

Figure 4.18 Linear Portion of Stress-Strain Curve of 3DRMC (Warp Direction)

4.2.4.3 Impact Properties

Drop weight impact test was conducted on both 3DRMC and 3DCMC. The impact velocity was approximately 3 m/s. Two specimens of each type were tested. Table 4.7 lists the number of strikes necessary to perforate each specimen and the total energy absorbed by each specimen. Table 4.8 lists the incident velocity of each strike for all the specimens tested, table 4.9 lists the velocity change of each strike, table 4.10 lists the residual velocity of each strike, and table 4.11 lists the energy dissipation of each strike.

On average, 3DCMC required more strikes to perforate than 3DRMC, i.e. 3DCMC absorbed more energy than 3DRMC. Carlson et al [13] and Qiu et al [60] found the same trend. They found that the porous composites have higher impact resistance than 3DRMC at low speed impact velocity. Therefore the higher energy absorption of 3DCMC may be explained by the presence of microcells across their structure. The 3DRMC had resin pockets full with epoxy resin in which cracks could easily propagate. Therefore 3DCMC excels 3DRMC in impact resistance. This property makes 3DCMC attractive for applications that require high impact resistance and low density.

Figure 4.19 shows the peak force over multiple strikes for each specimen tested. Figure 4.20 shows the average energy dissipated for each specimen tested.

Table 4.7 Number of Strikes Necessary to Perforate Each Specimen and Total Energy Absorbed (J)

Specimen	Number of Strikes for Perforation	Total Energy Absorbed (J)
Regular 3	8	136
Regular 4	7	57
Cellular 3	7	147
Cellular 4	3	113

Table 4.8 Incident Velocity (m/s) of each Strike for All Specimens

Specimen	Strike #1	#2	#3	#4	#5	#6	#7	#8
Regular 3	-3.11	-3.15	-3.14	-3.15	-3.14	-3.00	-3.01	
Regular 4	-3.11	-3.09	-3.13					
Cellular 3	-3.00	-3.08	-3.08	-3.07	-3.10	-3.04	-3.13	-3.06
Cellular 4	-3.00	-3.02	-3.01	-3.05	-3.06	-3.09	-3.11	

Table 4.9 Velocity Change (m/s) of Each Strike for All Specimens

Specimen	Strike #1	#2	#3	#4	#5	#6	#7	#8
Regular 3	5.07	5.13	5.27	5.16	3.45	4.25	3.13	
Regular 4	4.70	4.50	3.00					
Cellular 3	5.24	5.32	4.61	4.91	4.78	4.54	4.07	2.89
Cellular 4	5.13	5.49	4.19	5.56	5.32	3.90	3.03	

Table 4.10 Residual Velocity (m/s) of Each Strike for All Specimens

Specimen	Strike #1	#2	#3	#4	#5	#6	#7	#8
Regular 3	1.95	1.98	2.13	2.00	0.31	1.24	0.12	
Regular 4	1.59	1.41	-0.13					
Cellular 3	2.24	2.25	1.53	1.84	1.68	1.51	0.93	-0.18
Cellular 4	2.13	2.47	1.17	2.51	2.26	0.81	-0.08	

Table 4.11 Energy Dissipation (J) of each Strike for All Specimens

Specimen	Strike #1	#2	#3	#4	#5	#6	#7	#8
Regular 3	16.21	16.4	14.7	16.3	26.8	20.5	24.9	
Regular 4	19.5	20.6	26.9					
Cellular 3	10.9	12.1	19.6	16.6	18.6	19.1	24.6	25.7
Cellular 4	12.3	8.3	21.2	8.2	11.7	24.4	26.5	

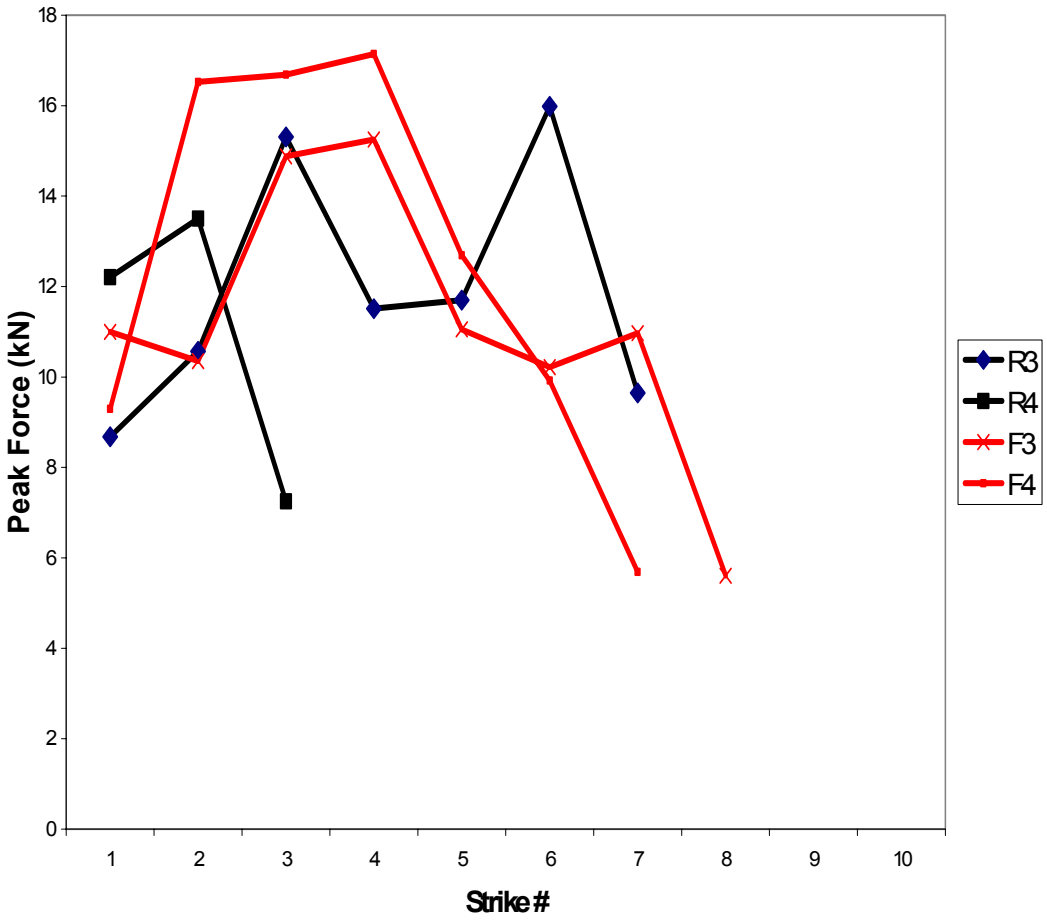

Figure 4.19 Peak Force over Multiple Strikes for Each Specimen Tested

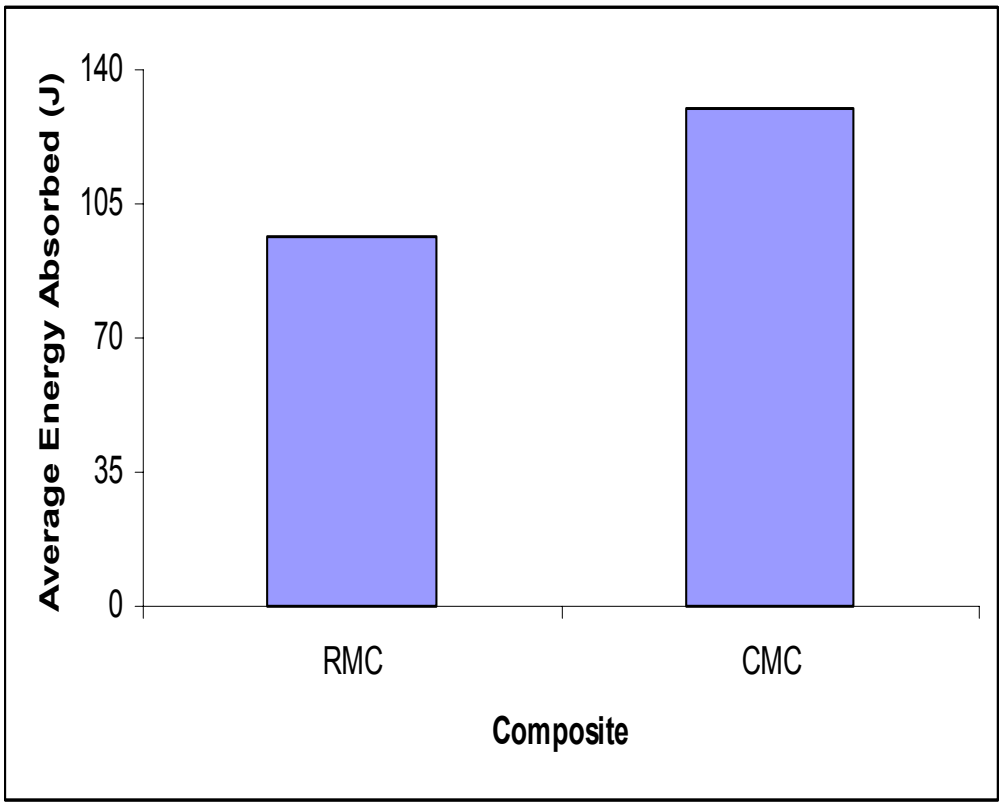

Figure 4.20 Total Energy Absorbed by 3DCMC and 3DRMC

5. CONCLUSIONS

The production time for fabricating 3DCMC by a physical blowing agent was successfully shortened from 20 hours to six hours. The process remains costly and expensive due to the high pressure vessel used. This led to the search for an alternative method and composites were successfully foamed using sodium bicarbonate as chemical blowing agent.

3DCMC were fabricated with different concentrations of sodium bicarbonate, which ranged from 2.5% to 25%. It has been demonstrated that the higher the concentration of the blowing agent, the higher the density reduction.

An optimum concentration of 5% was selected and composite samples were fabricated using this concentration. Four point bending test, tensile test and impact test were conducted.

3DCMC demonstrated similar flexural strength to 3DRMC, higher tangent modulus, and higher energy absorption under the low velocity drop weight impact test. There was no significant difference in tensile strength and modulus between 3DCMC and 3DRMC.

The same structure, which used to be fabricated in twenty hours using an expensive and dangerous high pressure vessel, can now be fabricated safely in two hours at atmospheric pressure using conventional ovens. The new process attained a higher productivity rate. Therefore this study was able to modify and optimize the 3DCMC process. The process is now ready to be transferred and applied in the industry.

6. RECOMMENDATIONS FOR FUTURE STUDY

The selection of an appropriate chemical blowing agent is a crucial step and can be time consuming. Several blowing agents were considered in this study and sodium bicarbonate was selected. However, it is to be mentioned that sodium oxide was retained in the composite structure. It would be imperative to search for a blowing agent, which leaves no residuals after its decomposition.

The foam properties depend on the blowing agent used. Therefore, a study could be done to compare composites foamed with different blowing agents.

Different applications require different properties. For example, the strength needed for a tennis racquet is lower than the strength needed for an airplane. Therefore, it may be imperative to test the mechanical properties of composites fabricated under different concentrations of the blowing agent, since higher concentrations would result in higher density reduction. Therefore, the designer would be able to choose an optimum concentration depending on the final application of the composite, which would offer an optimum weight and strength.

The curing temperature used in this study was 150°C. The curing temperature used for conventional vacuum bags is 100°C. It would be interesting to compare the mechanical properties of 3DCMC foamed under 150°C and conventional 3DRMC fabricated under 100°C. If there is substantial difference, then it may be imperative to investigate the possibility of applying a chemical blowing agent to foam 3DCMC under 100°C instead of 150°C.

7. REFERENCES

1. Xu, W. "Development and Analysis of Three-Dimensionally Reinforced Cellular Matrix Composites. " Ph.D. Dissertation, North Carolina State University, 2000.
2. Goel, S. K., and E. J. Beckman. "Generation of Microcellular Polymeric Foams Using Supercritical Carbon Dioxide. I: Effect of Pressure and Temperature on Nucleation." *Polymer Engineering and Science* 34, no.14 (1994): 1137-47.
3. Goel, S. K., and E. J. Beckman. "Generation of Microcellular Polymeric Foams Using Supercritical Carbon Dioxide. II: Cell Growth and Skin Formation." *Polymer Engineering and Science* 34, no.14 (1994): 1148-56.
4. Colton, J.S., and N.P.Suh. "The Nucleation of Microcellular Thermoplastic Foam with Additives: Part I: Theoretical Considerations." *Polymer Engineering and Science* 27, no. 7 (1987): 485-92.
5. Colton, J.S., and N.P.Suh. "The Nucleation of Microcellular Thermoplastic Foam with Additives: Part II: Experimental Results and Discussion." *Polymer Engineering and Science* 27, no. 7 (1987): 485-92.
6. Shell Chemical Company. Shell Chemical Company Literature, Technical Bulletin No.: SC 856-94.
7. Mohamed, M., and Z.Zhang, inventors. US Patent, 5,085,252.1992.
8. Mohamed, M., and A. K. Bilisik, inventors. US Patent, 5,465,760. 1995.
9. Mohamed, M. H., Z. Zhang, and L. Dickinson. "Manufacture of Multi-Layer Woven Preforms." *Advanced Composites and Processing Technology*

Presented at the Winter Annual Meeting of the ASME. American Society of Mechanical Engineers, Materials Division-MD, no.5 V5: 81-89. New York, NY, USA: American Society of Mechanical Engineers, 1988.

10. Brandt, J., K. Drechesler, M. Mohamed, and Pu Gu. "Manufacture and Performance of Carbon/Epoxy 3-D woven Composites." 37th *International SAMPE Symposium*, 864-77 Covina, Ca: SAMPE, 1992.
11. Dickinson, L., M. Mohamed, and E. Klang. "Impact Resistance and Compressional Properties of Three-Dimensional Woven Carbon/Epoxy Composites." *Developments in the Science and Technology of Composite Materials*. Editors ed., J. Fuller, G. Gruniger, K. Schulte, R. Bunsell, and A. MassiahLondon: Elsevier Applied Science, 1990.
12. Mohamed, M., C.Carlson, P. Gum, and R. Sadler. "Effect of Machining on the Perfomance of Carbon/Epoxy Composites. "International Conference on Advanced Composite Materials, 123-728. *Advanced Composites* 93, 1993.
13. Carlson, C. "The Influence of Matrix Modification on the Properties of 3-D Woven Carbon Composites." Ph.D. Dissertation, North Carolina State University, 1995.
14. Carlson, C., M. Mohamed, and R. Sadler. "Influence of Microballoons with the Matrix in 3-D Woven Carbon/Epoxy Composites." *Society for the Advancement of Material and Process Engineering* 38 (1993): 1892-902.
15. Mohamed, M. "Three-Dimensional Textiles." *American Scientist* 78 (1990): 530-541.

16. Gu, Pu. "Analysis of 3-D Woven Preforms and Their Composite Properties. " Ph.D. Dissertation, North Carolina State University, 1994.

17. Aronhime, M. T., and J. K. Gillham. "Time-Temperature-Transformation (TTT) Cure Diagram of Thermosetting Polymeric System." *In Advances in Polymer Science*, Epoxy Resin and Composites III. Editor K. Dusek, 84-113. Vol. 78. New York: Springer, 1986.

18. Dutta, A, and M. Cakmak. "Foaming of Vulcanized PP/EPDM Blends Using Chemical Blowing Agents." In *Rubber-Chemistry-and-Technology* 65 (1992): 778-791, 1992.

19. Liu, G., C. Park, and J. Lefas. "Production of Low-Density LLDPE Foams in Rotational Molding." *In Rubber-Chem-Technol* 65 n 4 (1992): 778-791.

20. Xanthos, M., Q. Zhang, S. K. Dey, Y. Li, and U. Yilmazer. "Effects of Resin Rheology on the Extrusion Foaming Characteristics of PET "*Journal-of-Cellular-Plastics* 34 n 6 (1998): 498-510.

21. Ghazali, Z., A.F Johnson, and K.Z Dahlan. " Radiation crosslinked Thermoplastics Natural Rubber." *Radiation-Physics-and-Chemistry* 55 n 1(1999): 73-79.

22. Bergounhon, P., and B. Ernst. "Plastisol Foams - Rheological and Rheo-Optical Approach to Developing New Grades of Poly (Vinyl Chloride)." *Plastics, -Rubber-and-Composites-Processing-and-Applications* 28 n 7 (1999): 317-320.

23. Zee, R.H., and C. Hsieh. "Energy Loss Partioning during Ballistic Impact of Polymer Composites." *Journal-of-Cellular-Plastics* 34 n 6 (1998): 300-310.

24. Pochiraju, Kishore, T. W. Chou, and Bharat M. Shah. "Experimental Characterization of 3-D Woven and Braided Composites. "*Proceedings of the 1996 Conference*. Part 2 (of 4). Collection of Technical Papers-AIAA/ASME/ASCE/AHS/ASC Structures, Structural Dynamics, and Materials Conference, no. 2 (1996): 908-915. New York, NY, USA: AIAA.
25. ASTM. "ASTM Designation: D 3039/D 3039M -95a. Standard Test Method for Tensile Properties of Polymer Matrix Composite Materials." *Annual Book of ASTM Standards.* West Conshohocken, PA: American Society for Testing and Materials, 1995.
26. ASTM. "ASTM Designation: D 6272 -00. Standard Test Method for Flexural Properties of Unreinforced and Reinforced Plastics and Electrical Insulating Materials." *Annual Book of ASTM Standards*. West Conshohocker, PA: American Society for Testing and Materials, 1998.
27. Clarke, D.R., S. Suresh, and I.M. Ward FRS. "An Introduction to Composite Materials". *Cambridge University Press*, 2nd Edition, 1996.
28. Kirt-Othmer. "Foamed Plastics." In *Encyclopedia of Chemical Technology*, Vol.11. 4th ed., New York, NY: John Wile & Sons, Inc., 1994.
29. Park, H., and J. R. Youn. " Study on Reaction Injection Molding of Polyurethane Microcellular Foam." *Polymer Engineering and Science* 35, no. 23 (1995): 1899-906.
30. Galy, J., A. Sabra, and J. -P. Pascault. "Characterization of Epoxy Thermosetting Systems by Differential Scanning Calorimetry." *Polymer Engineering and Science* 33, no. 18 (1993): 1157-64.

31. Fitzgerald, T.J., and A. Mortensen. “Processing of Microcellular SiC Foams. Part I Curing Kinetics of Polycarbosilane in Air.” *Journal of Materials Science* 30 (1995): 1025-32.
32. Vishay Measurements Group 91992) Student Manual for Strain Gage Technology.
33. Baldwin, D. F., C. B. Park, and N. P. Suh. “ A Microcellular Processing Study of Poly (Ethylene Terephthalate) in the Smorphous and Semicrystalline States. Part I: Microcell Nucleation. “*Polymer Engineering and Science* 36, no. 11 (1996): 1437-45.
34. Baldwin, D. F., C. B. Park, and N. P. Suh. “ A Microcellular Processing Study of Poly (Ethylene Terephthalate) in the Smorphous and Semicrystalline States. Part II: Microcell Nucleation. “*Polymer Engineering and Science* 36, no. 11 (1996): 1446-53.
35. Scriven, L. E. “On the Dynamics of Phase Growth.” *Chemical Engineering Science 10*, no. ½ (1959): 1-13.
36. Barlow, E. J. and W. E. Lanlois. “Diffusion of Gas From a Liquid into an Expanding Bubble.” *IBM Journal* (1962): 329-37.
37. Rosner, D. E., and M. Epstein. “Effects of Interface Kinetics, Capollarity and Solute Diffusion on Bubble Growth Rates in Highly Supersaturated Liquids.” *Chemical Engineering Science* 27 (1972): 69-88.
38. Ramesh, N. S., D. H. Rasmussen, and G. A. Campbell. “Numerical and Experimental Studies of Bubble Growth During the Microcellular Foaming Process.” *Polymer Engineering and Science* 31, no.23 (1991): 1657-84.

39. Amon, M., and C. C. Denson. “A Study of the Dynamics of Foam Growth: Analysis of the Growth of Closely Spaced Spherical Bubbles.” *Polymer Engineering and Science* 24, no.13 (1984): 1026-34.
40. Arefmanesh, A., and S. G. Advani. “Modeling of Bubble Growth in Viscoelastic Foams.” *In Processing of Polymers and Polymeric Composites*. Editors A. A. Tseng, and S. K. Suh, 185. Vol. 19. New York: ASME, 1990.
41. Arefmanesh, A., and S. G. Advani. “Diffusion-Induced Growth of a Gas Bubble in a Viscoelastic Fluid.” *Rheologica Acta* 30 (1991): 274-83.
42. Parks, K. L., and E. J. Beckman. “Generation of Microcellular Polyurethane Foams via Polymerization in Carbon Dioxide. I: Phase Behavior of Polyurethane Precursors.” *Polymer Engineering and Science* 36, no. 19 (1996): 2404-16.
43. Ramesh, N. S., and Nelson Malwitz. “Bubble Growth Dynamics in Olefinic Foams”. *Polymer Preprints, Division of Polymer Chemistry, American Chemical Society* 37, no. 2 (1998): 783-84.
44. Kumar, V., and J. E. Weller. “A Model for Unfoamed Skin on Microcellular Foams.” *Polymer Engineering and Science* 34, no. 3 (1994): 169-73.
45. Goel, S. K., and E. J. Beckman. “Nucleation and Growth in Microcellular Materials: Supercritical CO_2 As Foaming Agent*.” AIChE Journal* 41, no. 2 (1995): 357-67.
46. Baldwin, D. F., M. Shimbo, and N. P. Suh. “The Role of Gas Dissolution and Induced Crystallization During Microcellular Polymer Processing: A Study of

Poly (Ethylene Terephthalate) and Carbon Dioxide Systems." *J. Eng. Mat. & Tech., Transaction of the ASME* 117 (1995): 62-74.

47. Baldwin, D. F., C. B. Park, and N. P. Suh. "An Extrusion System for the Processing of Microcellular Polymer Sheets: Shaping and Cell Growth Control*." Polymer Engineering and Science* 36, no. 10 (1996): 1425-35.
48. Lee, S. T., and N.S Ramesh. "Study of Foam Sheet Formation. Part III: Effect of Foam Thickness and Cell Density." *In Cellular and Microcellular Materials, American Society of Materials Engineers*, MD Vol. 76. Editors V. Mumar, and K. A. Seeler, 71-80. New York: ASME, 1996.
49. Shafi, M. A., K. Joshi, and R. W. Flumerfelt. "Bubble Size Distribution in Freely Expanded Polymer Foams." *Chemical Engineering Science* 52, no.4 (1997): 635-44.
50. Shafi, M. A., and R. W Flumerfelt. "Initial Bubble Growth in Polymer Foam Processes." *Chemical Engineering Science* 52, no. 4 (1997): 627-44.
51. Joshi, K., J. G. Lee, M. A. Shafi, and R. W Flumerfelt. "Prediction of Cellular Structure in Free Expansion of Viscoelastic Media*." Journal of Applied Polymer Science* 67 (1998): 1353-68.
52. Kim, D. J, S. W. Kim, H.J Kang, and S. H Seo. "Foaming of Aliphatic Polyester Using Chemical Blowing Agent." *Journal of Applied Polymer Science* 81 no. 10 (2001): 2443-54.
53. Masahiro, O. "Polymeric Foaming in the New Century." Nihon Energy Gakkaishi *Journal of the Japan Institute of Energy* 79 no 10 (2000): 984-991.

54. Jung, L., and Y. C. Hsiung. " Rotational Molding of Expanded Polyethylene by *Pellets." Cellular Polymers 19*. no. 4 (2000) 257:70.

55. Chanjoong, K., and Y.J. Ryoun. "Environmentally Friendly Processing of Polyurethane Foam for Thermal Insulation." *Polymer Plastics Technology and Engineering* 39 no. 1 (2000): 163-85.

56. Kiatkamjornwong, S., S. Thinakorn, and P. Tasakorn. "Foaming Conditions of High Density Polyethylene-Natural Rubber Blends." *Plastics Rubber and Composites* 29 no. 4 (2000): 177-86.

57. Balasundharam, Sri. "Ballistic Behavior of 3-D Fabrics." M.S Thesis, North Carolina State University, 1999.

58. Flanagan, M. P., M. A. Zikry, J.W. Wall, and A.El-Shiekh. "An Experimental Investigation of High Velocity Impact and Penetration Failure Modes in Textile Composites." Journal of Composite Materials 33, no. 12 (1999): 1080:1103.

59. 3TEX, INC "Preform Process Specification", Proprietary.

60. Qiu, Y., W. Xu, Y.Wang, M. A. Zikry, and M. H. Mohamed. " Fabrication and Characterization of Three-Dimensional Cellular-Matrix Composites Reinforced With Woven Carbon Fabric." *Composite Science and Technology* 61, no.16 (2001): 2425-2435.

8. APPENDICES

APPENDIX A

A.1 Calculation of Density

Each sample was weighed and the mass was reported in grams. The volume of the samples was measured via the water displacement method. Each sample was placed in a cylindrical tube, which had 100 ml of water initially. The volume was recorded, after one minute in ml, which is equivalent to cm^3.

The density was calculated by dividing the mass by the volume and reported in g/cm^3.

A.2 Calculation of Fiber Volume Fraction

The volume of the fibers was calculated by dividing the mass of glass fabric retained after the ignition test by the density of fiberglass (2.62 g/cm^3). Finally the fiber volume fraction was determined by dividing the volume of fibers by the total volume of the composite.

APPENDIX B

B.1 Calculation of Flexural Strength

For load span of one third the support span:

$S = PL / bd^2$ where: (B.1)

S = stress in the outer fiber throughout the load span, MPa,

P = load at a given point on the load-deflection curve, N.

L = Support span, mm.

b = width of beam, mm.

d = depth of beam, mm.

Let P = Maximum load,

Therefore, the corresponding S would be the flexural strength.

B.2 Calculation of Tangent Modulus

For load span of one third the support span:

$E_B = 0.17 L^3m / bd^3$ where: (B.2)

E_B = modulus of elasticity in bending, MPa.

L = support span, mm.

b = width of beam, mm.

d = depth of beam, mm.

m = slope of the initial straight-line from the load deformation curve.

APPENDIX C

C.1 Tensile Strength

$(\sigma) = \frac{F}{A}$, Where: (C.1)

σ = Stress, MPa

F = Load, N

A = width of beam * depth of beam, mm^2.

For the tensile strength, maximum load at failure is substituted in the above equation.

C.2 Tensile Modulus

$E = \frac{\sigma}{\varepsilon}$, Where: (C.2)

E= Tensile Strength, GPa.

ε is the strain, which is reported through the strain gage.

Therefore, E is calculated as the slope of the stress strain curve.